Journal of the

OPTICAL SOCIETY *of* AMERICA

VOLUME 33
No. 5

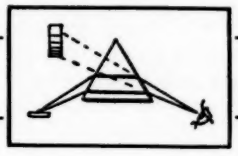

MAY
1943

Plate Calibration Problems . . . . . R. A. SAWYER AND H. B. VINCENT 247

Mathematics of Turbid Media . . . . . SEIBERT Q. DUNTLEY 252

Wave-Length Calibration of Spectrophotometers . . . . . J. A. VAN DEN AKKER 257

Metric for Colorspace . . . . . PARRY MOON AND DOMINA EBERLE SPENCER 260

Metric Based on the Composite Color Stimulus . PARRY MOON AND DOMINA EBERLE SPENCER 270

Empirical Approach to Lens Designs. The Huygens Eyepiece . . . . . W. M. STEMPEL 278

Book Review . . . . . A. G. HALL 269

Published monthly
at Prince and Lemon Sts., Lancaster, Pa.
by the
AMERICAN INSTITUTE OF PHYSICS
Incorporated
175 Fifth Avenue, New York, N. Y.
FOR AND UNDER THE EDITORIAL SUPERVISION OF THE
OPTICAL SOCIETY OF AMERICA

BOSTON UNIVERSITY
COLLEGE OF LIBERAL ARTS
LIBRARY

THE OPTICAL SOCIETY OF AMERICA

Officers of the Society

A. G. WORTHING, *President*
University of Pittsburgh
Pittsburgh, Pennsylvania

A. H. PFUND, *Vice President*
Johns Hopkins University
Baltimore, Maryland

ARTHUR C. HARDY, *Secretary*
Massachusetts Institute of Technology
Cambridge, Massachusetts

W. W. GRAEPER, *Treasurer*
Bausch & Lomb Optical Company
Rochester, New York

The Board of Directors consists of the above officers; the Editor of the Journal; the Past President; and five directors-at-large.

K. S. GIBSON, *Past President*
National Bureau of Standards
Washington, D. C.

GEORGE R. HARRISON, *Editor*
Massachusetts Institute of Technology
Cambridge, Massachusetts

Directors-at-Large

J. W. BEAMS
University of Virginia
Charlottesville, Virginia

D. B. JUDD
National Bureau of Standards
Washington, D. C.

RUDOLF KINGSLAKE
Eastman Kodak Company
Rochester, New York

D. L. MACADAM
Eastman Kodak Company
Rochester, New York

R. A. SAWYER
University of Michigan
Ann Arbor, Michigan

Rochester, New York, Section

J. H. WEBB, *President*
G. H. AKLIN, *Vice President*
A. F. TURNER, *Secretary*
F. H. PERRIN, *Treasurer*

Councillors:

F. E. ALTMAN
J. W. FORREST
F. M. E. HOLMES
V. L. PARKS
R. B HORSFALL (*ex officio*)

Patrons

AMERICAN OPTICAL COMPANY BAUSCH & LOMB OPTICAL COMPANY
EASTMAN KODAK COMPANY

Corporation Members

AMERICAN CYSTOSCOPE MAKERS, INC., New York, New York
AMERICAN OPTICAL COMPANY, Southbridge, Massachusetts
BAUSCH & LOMB OPTICAL COMPANY, Rochester, New York
BELL & HOWELL COMPANY, Chicago, Illinois
BELL TELEPHONE LABORATORIES, INC., New York, New York
BENDIX AVIATION CORPORATION, New York, New York
CORNING GLASS WORKS, Corning, New York
E. I. DUPONT DE NEMOURS & COMPANY, INC., Chemical Department, Experimental Station, Wilmington, Delaware
EASTMAN KODAK COMPANY, Rochester, New York
FAIRCHILD AVIATION CORPORATION, Jamaica, New York
FISH-SCHURMAN CORPORATION, New York, New York
GAERTNER SCIENTIFIC CORPORATION, Chicago, Illinois
W. & L. E. GURLEY, Troy, New York
INTERCHEMICAL CORPORATION, New York, New York
KEUFFEL & ESSER COMPANY, Hoboken, New Jersey
NATIONAL CARBON COMPANY, Cleveland, Ohio
PERKIN-ELMER CORPORATION, Glenbrook, Connecticut
POLAROID CORPORATION, Cambridge, Massachusetts
PORTMAN MACHINE TOOL COMPANY, New Rochelle, New York
SIMPSON OPTICAL MANUFACTURING COMPANY, Chicago, Illinois
SPENCER LENS COMPANY, Buffalo, New York
ARTHUR H. THOMAS COMPANY, Philadelphia, Pennsylvania

THE OPTICAL SOCIETY OF AMERICA was organized in 1916 "*to increase and diffuse the knowledge of optics in all its branches, pure and applied, to promote the mutual interests of investigators of optical problems, of designers, manufacturers and users of optical instruments and apparatus of all kinds and to encourage cooperation among them.*" It aims to serve the interests of all who are engaged in any branch of optics from fundamental research to the manufacture of optical goods.

MEMBERSHIP

Regular Members: "Any person who has contributed materially to the advancement of optics is eligible for regular membership."

Associate Members: "Any person who is interested in optics is eligible for associate membership."

Corporate Members: "Any corporation desirous of encouraging the work of the Society is eligible for corporation membership."

Patrons: The payment, within any one year, of $1000 or more toward the expenses of the Society by any corporation or individual entitles such corporation or individual to the rank of patron.

The Society cordially invites to membership all who are interested in any branch of optics, either in research, in instruction, in optical or illuminating engineering, in the manufacture and distribution of optical goods of all kinds or in physiological and medical optics.

ANNUAL DUES

Regular members, $8.50; Associate members, $6.00; Corporate members, $50.00; Patrons, $1000.00. These dues include subscription to the Society's official journal, the *Journal of the Optical Society of America*.

CHANGES OF ADDRESS

All changes of address of members of the Optical Society of America should be communicated to the Secretary, Professor Arthur C. Hardy, Massachusetts Institute of Technology, Cambridge, Massachusetts.

Journal of the
OPTICAL SOCIETY
of AMERICA

VOLUME 33, NUMBER 5 MAY, 1943

Plate Calibration Problems*

R. A. SAWYER AND H. B. VINCENT
*University of Michigan, Ann Arbor, Michigan***

IN modern spectrochemistry, with its increasing demands for accuracy and speed, precise emulsion calibration is becoming increasingly necessary. Precision is especially vital if lines of rather unequal intensity are to be compared, and particularly if, as is often the case, with the use of light sources of not too constant intensity.

Numerous studies have been published of emulsion calibration problems and of particular calibration techniques. Survey of the literature, however, reveals the use even today of incorrect techniques and instances of failure to verify the consistency of the methods used. Certainly no calibration method should be used without a check of its self-consistency. A simple procedure for the purpose has been pointed out by Harrison and has been described in a recent paper by H. H. Grossman and the authors.[1] Briefly it is only necessary to plot two curves, obtained by the method under test, from records on the same plate, made under identical conditions except that the light intensity is varied between the two sets of observations in any way which does not affect its size, color-temperature, or continuity. The calibration method is self-consistent if the two resulting curves when plotted on the same coordinate axes against the same set of intensity values result in two curves which can be translated into one another by the same displacement, parallel to the intensity axis, of each point on one curve.

In the course of the present study of calibration procedures, various calibration methods have been examined. The purpose was to find a method which satisfies the above self-consistency test, is relatively simple to use, and is applicable to both line and continuous light sources. Any technique used should of course provide equal time of exposure for all steps of the calibration scale and, if possible, this time should be the same as that of the exposures to be evaluated. This equality of time is necessitated by the well known reciprocity law failure to which all emulsions are subject to a greater or less degree.

Connected with the reciprocity law is the effect shown by many plates in responding differently to an intermittent than to a continuous exposure —the "intermittency effect." This effect must be considered if any light source is used, either in calibration or for intensity measurements, which is operated from the 60-cycle lighting circuit or from any other discontinuous supply. Trouble can be avoided in such cases by arranging to make the calibration by some self-consistent method which uses the same light source, or at least has the same intermittency as the source on which measurements are to be made. The inter-

* Presented at the Tenth Summer Conference on Spectroscopy and its Applications at Massachusetts Institute of Technology, Cambridge, Massachusetts, July 20–22, 1942.

** The work reported here was done in the Department of Physics on a project sponsored through the Department of Engineering Research.

[1] H. H. Grossman, R. A. Sawyer, and H. B. Vincent, J. Opt. Soc. Am. **33**, 185 (1943).

BOSTON UNIVERSITY
COLLEGE OF LIBERAL ARTS
LIBRARY

mittency-law effect must be considered particularly in the use of the rotating step-sector, or the logarithmic-sector for plate calibration. Because of its relative simplicity, the rotating sector has been widely used and is supplied by most makers of spectrographic equipment. Some years ago Ornstein and his co-workers cast doubt on the validity of the rotating sector because of the intermittency effect difficulties.

More recently, however, O'Brien,[2] and also Webb,[3] have stated that at sufficiently high speeds, intermittent exposures are wholly equivalent to continuous exposures. Unfortunately, O'Brien never published the details of his experiments, so it was impossible to repeat them in this work. Webb has asserted that at a flash frequency such that each silver grain should receive, on the average, not more than one quantum per light flash, the intermittency effect should vanish. He inferred from measurements showing decreasing effect with increasing frequency, that the intermittency effect should disappear in most practical spectroscopic applications at sector disk speeds of 3600 flashes per minute. With the equipment used in this work it has never been possible to verify this observation or prediction in the general case.

For emulsions with relatively small intermittency effect, such as those of the Cramer Contrast or the Eastman SA No. 1 plates, sector disk calibration curves, obtained at 3000 flashes per minute were found, within the accuracy of measurement, to be self-consistent and to check the calibration curves, also self-consistent, obtained by an inverse square procedure. For the popular Polychrome plate, however, flash rates up to 10,000 per minute failed to lead to self-consistent calibration curves. Furthermore, speeds of 1500 to 5000 flashes per minute gave, as closely as could be determined, the same curve as was obtained at 10,000 flashes per minute and there was no indication that higher speeds would lead to a true calibration curve.

In Fig. 1, are shown the emulsion calibration curves obtained with the laboratory equipment by several different procedures. A large Bausch and Lomb quartz spectrograph was used and

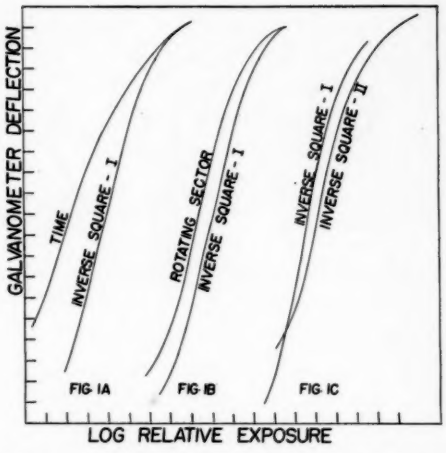

FIG. 1. Calibrations curves obtained for Polychrome emulsion by (A) time variation of exposure; (B) rotating sector; (C) inverse method using lamp without diffuser (II), compared in each case with self-consistent curve (I) obtained with inverse square method using lamp and diffuser.

measurements were made with the laboratory microphotometer at 4202A on the spectra from a battery-operated tungsten filament lamp. All the curves in the figure were obtained with Eastman Polychrome emulsion. In curve *A* a simple time variation of exposure was used to demonstrate any reciprocity-law failure. The exposures of curve *B* were obtained with rotating sectors of different aperture with 10,000 interruptions of the beam per minute. As indicated above, these two curves are quite different, and neither of them is found to be self-consistent.

The present experiments have not been extensive enough to indicate fully the limits within which the rotating sector can be used. The validity of the method may depend on the spectrographic equipment used; it certainly depends on the emulsion and possibly on the microphotometer light losses, and in any case the microphotometer precision has a determining effect on the decision as to whether the calibration curve in question is sufficiently near self-consistency. The rotating-sector method is undoubtedly adequate for certain conditions and for plates with low reciprocity-law failure; it may be sufficiently good in other cases where too high precision is not demanded or obtained. Unquestionably, however, everyone who uses the rotating sector

[2] B. O'Brien and V. L. Parks, Phys. Rev. **43**, 1052A (1933).
[3] J. H. Webb, J. Opt. Soc. Am. **23**, 157 and 316 (1933).

should apply a self-consistency test to his calibration curves before relying on them too heavily.

It has been possible under proper conditions to obtain self-consistent calibration curves by using the inverse square law of intensity variation to calculate the relative intensities of the calibrating exposures made at different slit-source distances. To use this calibrating technique the light source must be constant in intensity; it must also be small enough and must radiate uniformly enough over the light bundle used to be treated as a point source. The controlled spark source described elsewhere[4] meets these requirements. In some trials a diffusing screen has been used as a source. The screen, 5 mm square and placed at a fixed distance of about 25 cm from the slit, was illuminated by a light source, usually a tungsten filament lamp, placed at varying distances behind the screen. The diffuser has the advantage that it presents the same solid angle to the slit at all times and so avoids the possible source of error, that all areas of the optics may not image the rays in the same way. This danger is always present with the source at varying distances and hence using different areas of the spectrograph optics.

In the case of one of the spectrographs and spark sources tested in this work, the spark used without diffuser gave the calibration curve C-II, which is not self-consistent; a lamp and diffuser led to the inverse-square curves (I) in Fig. 1 (A, B, and C), which proved to be self-consistent. However, another spectrograph and spark source tested, although similar in design and characteristics, gave the spark without diffuser, a self-consistent calibration curve. The differences in behavior of the two sets of equipment were not analyzed but are probably due to transmission differences in different areas of the optics.

It should be noted that, in general, line and continuous sources may not give the same calibration curves for a given emulsion and wave-length. Furthermore for either type of source slight variations in self-consistency may be found from wave-length to wave-length. The differences probably arise from reflected light in the spectrograph and from Schwartschild-Villiger effect in the microphotometer, which may be quite different for continuous and for line spectra. To avoid these difficulties it is important to use the same type of source, and preferably the same source, in calibration that is used in the measurements to be reduced.

The inverse square method of calibration is not very convenient, since either the spectrograph or the light source must be moved between each pair of exposures in the calibration procedure, necessitating re-alignment of their relative positions, and possible errors if the optics area used in each exposure is not the same both in size and position.

These considerations, as well as the space requirements of the method, led to an examination of other methods of reducing exposure intensities reproducibly. A promising method, both in convenience and simplicity, seemed to be that of neutral filters. The results of experiments with this method, which will be described briefly, indicate that this method merits more consideration.

So far as is known, suitable neutral filters are not readily available on the market, although numerous types of absorbers or partial reflectors have been described in the literature. Several types of metallic films have been suggested for the purpose, including platinum, aluminum, and antimony. Antimony-film filters were described five years ago by Langstroth and McRae.[5] Such filters were, according to Harrison,[6] first used by Ornstein and are said to be quite closely neutral down to about 2500A.

Langstroth and McRae deposited their filters by burning antimony trihydride in an atmosphere of hydrogen. With the object of getting a more uniform and tenacious film, the films in the present work have been deposited on quartz plates by thermal evaporation in a vacuum. After a few experiments, it is possible to predetermine the transmittance of the film fairly closely. In the present case it was desired to have at least eight steps on the calibration curve. Four filters were determined on to have transmissions of approximately 65 percent, 50 percent, 35 percent, and 15 percent. The final values

[4] R. A. Sawyer and H. B. Vincent, *Proceedings of the Fifth Summer Conference on Spectroscopy* (Wiley, New York, 1938), p. 1.

[5] G. O. Langstroth and D. R. McRae, *Proceedings of the Fifth Summer Conference on Spectroscopy*, p. 105.

[6] G. R. Harrison, J. Opt. Soc. Am. **19**, 267 (1929).

actually obtained experimentally by inverse square measurement for the wave-length 4202A were 63.9 percent, 49.4 percent, 36.9 percent, and 15.4 percent. By combining the filters in various combinations, fifteen fairly well separated transmission steps were obtained as in Table I.

The filters were mounted in a cell, placed just before the spectrograph slit, so arranged that one, two, or three could be used at a time. They were, of course, always used in the position and order in which their transmissions had been determined previously with the help of the diffuser and inverse square law. A large Littrow quartz spectrograph was used with a battery-operated tungsten-filament lamp as a light source. The wave-length chosen for measurement was 4202A.

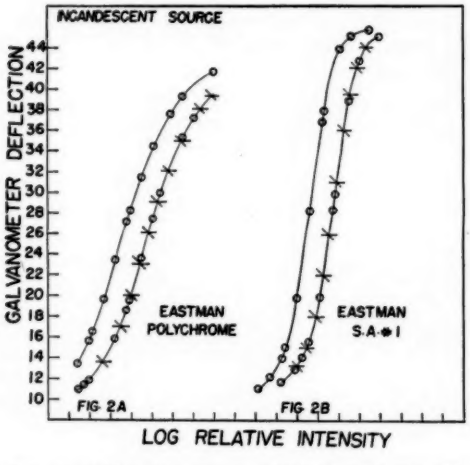

FIG. 2. Calibrations curves obtained with the aid of antimony filters for (A) Eastman Polychrome emulsion and (B) Emulsion Spectrum Analysis No. 1 emulsion. In each instance the crosses on the right-hand curve show points transposed from the left-hand curve by the intensity change corresponding to known filter transmission.

The results obtained for Eastman Polychrome emulsion are shown in Fig. 2A. The left-hand curve is made with the filter combinations at one source-slit distance, while the right-hand curve is made from observations at a longer distance. From the inverse square law the logarithm of the two intensity ratios is computed to be 0.35 and the crosses on the right-hand curve show points which have been transposed by this amount from the left-hand curve. It can be seen that the squares fit the curve practically as well as do the circles. The photometer galvanometer readings are shown in the left margin and from them the precision of the results can be seen. The fit of the square points on the right-hand curve indicates the self-consistency of the calibration, as well as of the inverse square procedure.

Similar observations on the Spectrum Analysis No. 1 emulsion are shown in Fig. 2B. The calibration curve is much steeper and the sensitivity to lack of self-consistency even greater. It will be seen, however, that the check for self-consistency is equally good. Similar filter calibration curves have been made for other emulsions, but the two examples given indicate sufficiently the validity of the method.

To keep the emulsion grain error low in this work a line length of about 5 mm was photometered. As a result, each point of the calibration curves is taken from a different spectrum, recorded on the same plate. The smoothness of the fit is an indication that (1) the variation in plate sensitivity from point to point is very small, and (2) the source variation is also small. The source variation has been, however, checked and corrected by measurements from a plate made simultaneously on another spectrograph on which, since all conditions are held constant, all spectra should have equal blackening, unless the source varies.

TABLE I.

Filters	Transmission (determined experimentally)
None	100%
1	63.9
2	49.4
3	36.9
1 & 2	34.9
1 & 3	26.2
2 & 3	19.8
4	15.4
1 & 2 & 3	14.2
1 & 4	11.0
2 & 4	8.54
3 & 4	6.60
1 & 2 & 4	6.31
1 & 3 & 4	5.44
2 & 3 & 4	4.85

The curves in Fig. 2 showing the filter-calibration curves for the Polychrome and S.A. No. 1 emulsions indicate the validity of the method. Similar curves have been made for other emul-

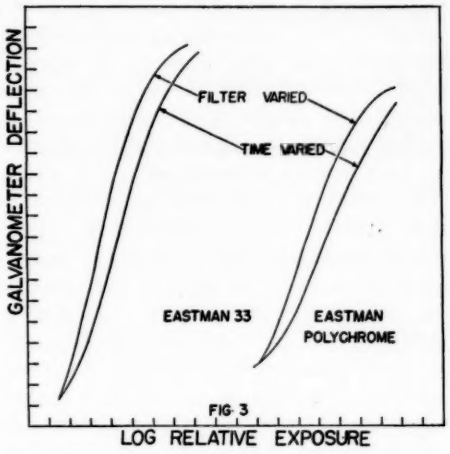

FIG. 3. Comparison of emulsion calibration curves made by time and by filter variation of intensity for Eastman 33 (left) and Eastman Polychrome (right) emulsions.

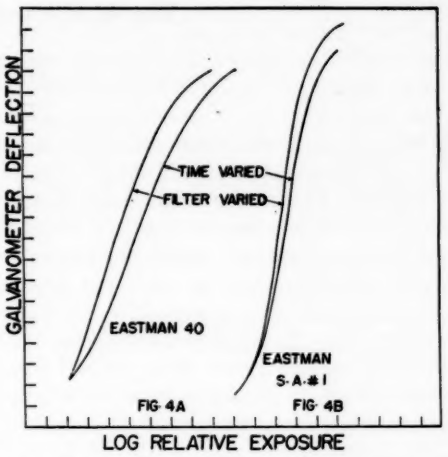

FIG. 4. Comparison of emulsion calibration curves made by time and by filter variation of intensity for Eastman 40 (left) and Eastman Spectrum Analysis No. 1 (right) emulsions.

sions. To illustrate the results obtainable with the filters, a few curves have been made to demonstrate the reciprocity law deviation for several emulsions for the wave-length 4202A. In these cases, the filter-calibration curve was made as previously described. The time-variation curve was made with a constant source at a fixed distance and with the time of exposure varied. In Fig. 3 are shown results obtained for Polychrome and Eastman 33 emulsions, while Fig. 4 shows similar data for the Eastman 40 and Spectrum Analysis No. 1 emulsions. The relative position of the pairs of curves is arbitrary.

It had been hoped to extend this work by checking the transmission of the filters and the validity of their use at several wave-lengths, both longer and shorter, and to make further studies of the rotating sector method in the hope of determining its limitations more exactly. The pressure of defense research in Ann Arbor and the absence of one of the writers from there has severely limited the work.

More quantitative spectroscopy than ever before is being practiced in this country, and the extent is probably limited only by the equipment obtainable. Precise calibration is essential to all good work. Most workers will wish if possible to utilize some quick method, such as a rotating sector-disk or the known relative intensities of several lines in a stabilized spectrum, such as the controlled iron spark. It is essential, however, to have methods of verifying the validity of the procedures used, or of establishing true calibration curves for reference purposes. It is hoped that every worker in the field will undertake the simple test outlined to check the validity of his present methods of emulsion calibration. A set of calibrated antimony filters offers a compact and convenient equipment for emulsion calibration. Their transmissions can be determined with sufficient accuracy for the present needs of spectrochemistry. The method can readily be applied to any spectrographic apparatus and is believed to be as satisfactory a procedure as is at present available.

The Mathematics of Turbid Media*

SEIBERT Q. DUNTLEY
Massachusetts Institute of Technology, Cambridge, Massachusetts

TO both mathematicians and physicists the passage of light through turbid media is an old problem. In 1871 Lord Rayleigh began his work on the scattering produced by small particles. The principle of "self-illumination" was recognized by Schuster in 1903, and later was applied by him to the special case of a self-luminous gas. Throughout succeeding years Schuster's equations have been applied to such commercial products as opal glass, photographic film, paint, paper, plastics, and textiles. Meanwhile, a completely general theory of turbid media, in terms of integral equations, was proposed in 1913 by King. Useful solutions of King's equations have never been produced, and, in effect, the general case remains unsolved. This paper* is an attempt to review the mathematical aspects of turbid media.

1. PRIMARY SCATTERING

Light is scattered in traversing any region of space containing particles which differ in refractive index from their surroundings. It is usually postulated that, in passing through an infinitesimal layer of the scattering medium included by two planes normal to the direction of the light, diminution due to scattering is proportional to the quantity of light present at the layer. Thus, $dI_x'/dx=-S'I_x'$. This has been called *primary scattering*. The coefficient of proportionality is referred to as the scattering coefficient. It is here denoted by S'.** Such reasoning leads to an exponential law of attenuation for radiation transmitted by the medium. ($T'=\epsilon^{-S'X}$.) In general, this equation is valid only when the light is monochromatic.

In the attenuation of a beam of light by scattering, no energy is actually lost. The scattering process merely re-directs it. Some materials, however, transform light into other kinds of energy, and such substances are said to possess absorption. Following the teachings of Bouguer, Lambert, and others, the diminution of monochromatic light in passing through an infinitesimal layer of a homogenous absorbing substance is proportional to the quantity of light reaching the layer. $dI_x'/dx=-\mu'I_x'$. Again, the proportionality constant is defined as the coefficient of absorption, and radiation is exponentially attenuated with the medium. ($T'=\epsilon^{-\mu'X}$.)

In the general case, a medium both scatters and absorbs radiation. A directed beam traversing an infinitesimal layer of such a material is diminished by both mechanisms in proportion to the quantity of light incident on the layer. Thus, $dI_x'/dx=-(\mu'+S')I_x'$. The equation deals only with the disappearance of energy from the original directed beam and is not concerned with any further interaction between the scattered light and the medium.

Most of the mathematical effort lavished on turbid media has been concerned with relating the scattering coefficient S' to other physical properties of the material. This was the approach of Rayleigh.[1] Due to his efforts and to those of many who have come after him, expressions have been derived evaluating the quality, quantity, and state of polarization of light scattered by spherical and ellipsoidal particles throughout all

* Invited paper, Symposium on Mathematics in the Field of Optics; joint session of the American Mathematical Society and the Optical Society of America, New York, October 30, 1942.

** The symbols used in this paper conform with the recommendations of the International Commission on Illumination (Neuvieme Session, 1937, p. 3) for the specification of opal glass. The following symbols will be used throughout the paper:

I' The unscattered residue of the primary beam at any depth x within the medium
μ The absorption coefficient for internal diffused flux
μ' The absorption coefficient for incident flux
S The total scattering coefficient for internal diffused flux
B The portion of S scattered backward
F The portion of S scattered forward
S' The total scattering coefficient for incident light
B' The portion of S' scattered backward
F' The portion of S' scattered forward
t The quantity of diffused flux moving in the forward direction
s The quantity of diffused flux moving in the backward direction
x Thickness coordinate
X Total thickness.

[1] Lord Rayleigh, Proc. Roy. Soc. **A90**, 219 (1914).

azimuths, in terms of their size, shape, relative refractive index, and electrical conductivity.

Theories of primary scattering adequately describe the observed behavior of scattering media containing comparatively few particles. For such materials the practical importance of scattering theory probably cannot be overemphasized. Indeed, it appears that the useful applications of these theories have barely been tapped. For instance, it should be pointed out that, in many cases, the wave-length of visible light bears somewhat the same relation to the size of the scattering particle as do x-rays to the ions and atoms by which they are diffracted. It seems likely that studies of primary scattering may yield useful information analogous to the results now obtained on amorphous substances by x-ray methods. In fact, the optical methods should prove more versatile because experimental techniques are much easier.

2. SECONDARY SCATTERING

When a turbid medium contains many scattering particles account must be taken of *secondary* or multiple rescattering of the permeating radiation. A statistical type of approach to the problem of secondary scattering was made by Weiner in 1900.[2] He considered separately all rays reaching a given point after N changes in direction. By summing up the contributions corresponding to various values of N he obtained multiple integrals which describe the optical properties of turbid media. Although this approach is direct, it has thus far not been possible to formulate the general problem in manageable form. In the field of meteorology, however, Weiner's method has been usefully applied by Koschmieder.[3]

The problem was more usefully formulated by Schuster,[4] who in 1903 published a theory of the effect of radiation on the transmission of heat through matter. Here he set forth very clearly the philosophy that every volume element within the medium receives scattered light from every other volume element. This has been called principle of *self-illumination*. In 1905, Schuster[5] published an historic paper describing the escape of radiation from the self-luminous foggy atmosphere of a star. He expressed the principle of self-illumination in terms of two diffused fluxes moving in opposite directions through the material, each contributing back-scattered flux to the other. Because some of the particles in a stellar atmosphere are self-luminous, his equations contain terms representing the emission of light by the gas. Let E denote the total energy radiated per second in a wave-length range between λ and $\lambda+d\lambda$ by a completely black unit surface. Schuster considered a thin parallel-sided slab within the star atmosphere, so chosen that the boundary surfaces were normal to the direction in which the escaping radiation is to be viewed. This is illustrated by Fig. 1 wherein t describes the diffused flux incident on the layer dx in the emergent direction, and s is that impinging on dx in the opposite direction. Since the scattering particles of the stellar atmosphere are gas molecules, Schuster rightfully considered half the scattered flux to go forward and half to go backward. He assumed that in passing through the layer dx, diffused flux would be increased by emitted light, decreased by absorption, diminished by that part of itself scattered to the rear, and augmented by back-scattered flux from the oppositely moving flux body. This situation is represented by the following simultaneous differential equations. Here, S represents the total scattering coefficient and μ represents the over-all absorption coefficient.

$$\frac{dt}{dx}=\mu E-\mu t-\tfrac{1}{2}St+\tfrac{1}{2}Ss,$$

$$-\frac{ds}{dx}=\mu E-\mu s-\tfrac{1}{2}Ss+\tfrac{1}{2}St.$$

Although these differential equations can be extended to represent the behavior of slabs of turbid media illuminated normal to their surfaces, the general case requires that illumination enter the medium from any direction. Therefore, Schuster's method treats only a special case of the general problem.

[2] C. Weiner, Nova Acta d. K. Leop. Carol Akad D. Naturf. Halle **73**, 1–240 (1900); and **91**, 1–292 (1909), **12**, 33–53 and 171–181 (1924).

[3] H. Koschmieder, Beitr. z. Phys. d. freien Atm. **12**, 33–35(1924) and **12**, 171–181 (1924).

[4] A. Schuster, Phil. Mag. **5**, 243 (1903).

[5] A. Schuster, Astrophys. J. **21**, 1 (1905).

3. THE INTEGRAL EQUATION METHOD

A key to a completely general approach was given by Jackson[6] in 1910. He showed that the generalized differential equations given by Schuster in 1903 can be transformed into an integral equation of the Fredholm type. This transformation appears to have encouraged King[7] to formulate the completely general treatment which he published in 1913. Here the

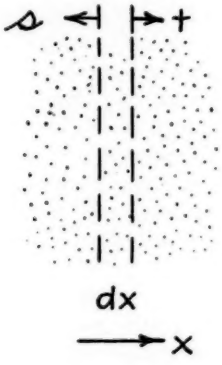

FIG. 1.

problem of turbid media is expressed in terms of a first-order integral equation of the second kind. This important work, described by Middleton[8] as "a paper of great formal elegance and considerable difficulty," seems seldom to be referred to in the literature. Therefore, it is appropriate to review the derivation of the integral equation due to King.

Suppose a region of space bounded by a limiting surface Σ (see Fig. 2) contains matter which both scatters and absorbs. Suppose this space to be irradiated by monochromatic light from an external source in such a manner that at any point O having coordinates x, y, z, there is a value of irradiance E which is understood to have both a magnitude and a direction. The flux scattered by a volume element dv containing the point O in a small solid angle $d\omega$ and in a direction making an angle θ with E is denoted by $I(x, y, z, 0, \theta)dvd\omega$. Of this flux an amount $S(\theta)E(x, y, z)dvd\omega$ is contributed by primary scattering. Here $S(\theta)$ represents the scattering coefficient in the direction θ. Additional scattered flux appears because of self-illumination. Thus, from any other volume element dv' at coordinates x', y', z' from which dv lies at a distance r' and in a direction θ' the illumination at dv will be denoted by $I(x', y', z', r', \theta')dv'd\omega r'^{-2}$. This illumination contributes to the radiation scattered from dv the amount $S(\widehat{rr'})I(x', y', z', r', \theta')dv'd\omega dvr'^{-2}$ where $\widehat{rr'}$ denotes the angle between r and r'. The total contribution to the scattered radiation from dv due to self-illumination is

$$d\omega dv\int_{\Sigma} S(\widehat{rr'})I(x', y', z', r', \theta')r'^{-2}dv',$$

where this integral is taken throughout the entire volume bounded by the surface Σ. It is proper that the primary and secondary fluxes be added, since their phases are completely random. Hence we have an integral equation for the radiation at and from any point:

$$I(x, y, z, 0, \theta)=S(\theta)E(x, y, z)+\int_{\Sigma} S(\widehat{rr'})I(x', y', z', r', \theta')r'^{-2}dv'.$$

This equation is not in usable form until a relation is established between $I(x', y', z', r', \theta')$ and $I(x', y', z', 0, \theta')$. This may readily be obtained by means of the differential equation for the diminution by primary scattering of flux from dv' in traversing an element of path dr'. Thus:

$$-d/dr'I(x', y', z', r', \theta')dv'd\omega dr' =(\mu+S)I(x', y', z', r', \theta')dv'd\omega dr'.$$

This has the solution:

$$I(x', y', z', r', \theta') =I(x', y', z', 0, \theta')\exp\left[-\int_0^{r'}(\mu+S)dr'\right].$$

Here the effect of self-illumination within $d\omega$ is neglected since it enters into the equation only to the second order of small quantities. The integral equation for the radiation at and from any point may now be written:

$$I(x, y, z, 0, \theta)=S(\theta)E(x, y, z)+\int_{\Sigma} S(\widehat{rr'})I(x', y', z', 0, \theta')r'^{-2}\times\exp\left[-\int_0^{r'}(\mu+S)dr'\right]dv'.$$

[6] W. H. Jackson, Bull. Am. Math. Soc. **16**, 473 (1910).
[7] L. V. King, Phil. Trans. Roy. Soc. London **A212**, 375 (1913).
[8] W. E. K. Middleton, *Visibility in Meteorology* (University Toronto Press, 1914).

After $I(x, y, z, 0, \theta)$ is found throughout the volume bounded by the surface Σ, the irradiance T reaching any point P within the boundary contained in a small solid angle is given by the relation

$$T\omega=\omega\int_0^{r_0} I(x, y, z, 0, \theta)\exp\left[-\int_0^r(\mu+S)dr'\right]dr,$$

where $r=PO$ and r_0 is the radius vector to the boundary.

Evidently this constitutes a completely general formulation of the problem, and it remains only to produce satisfactory solutions of this integral equation. Perhaps it is unfortunate that King chose to expend his efforts on a solution intended to describe the brightness of the sky, for he was forced to make certain simplifying assumptions which included neglecting the curvature of the earth. As a result, his equations do not lead to predictions in accordance with observation. It is regrettable that the failure of King's solution correctly to describe the brightness of the sky seems to have prevented the utilization of his integral equation for problems in which it appears there is more likelihood of success.

Although integral equations date from Abel's generalization of the tautochrome problem in 1823, and from Liouville's work in 1837, extensive engineering use of integral equation methods does not seem to have developed.* This may be due, in part, to the need for further work on the part of mathematicians. It still remains to produce useful solutions of King's equations for turbid media.

4. THE DIFFERENTIAL EQUATION METHOD

In the absence of a useful general treatment, the differential equation method of Schuster has been employed in several special cases. These include most of the turbid materials of interest to industry. The first direct attempt to produce a useful treatment for an industrially important turbid medium appears to have been the work of Channon, Renwick, and Storr[9] in 1918. Postulating only the conservation of energy principle, they showed by successive difference methods the form of equation which must be obeyed by sheets of opal glass under completely diffused illumination. They further showed that the form of these equations agreed with solutions obtained from the differential equations of Schuster provided the emission terms of those equations are set equal to zero.

The development of the differential equation type treatment was traced by the author in an earlier paper.[10] The solutions obtained by various authors differ in completeness and complexity according to the needs of the problem for which they were derived, but all are based on differential equations of the type proposed by Schuster. The principal innovations include additional terms to represent the entry into the medium of light from an external source, and removal of the restriction that half the scattered light be directed forward and half backward. The most complete and general theory of the Schuster type is represented by the following differential equations which refer to Fig. 3:

$$\begin{aligned} dI_x'/dx &= -(\mu'+B'+F')I_x', \\ dt/dx &= F'I_x'+\mu E-\mu t-Bt+Bs, \\ -ds/dx &= B'I_x'+\mu E-\mu s-Bs+Bt. \end{aligned}$$

These differential equations may be thought of as a steady state equation of continuity for flux

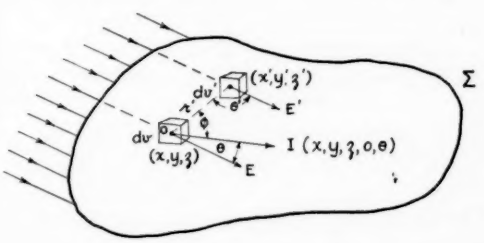

FIG. 2.

permeating the turbid medium. They involve the assumption that the radiation is monochromatic and the assumption that the medium may be divided laminarwise without destroying its over-all homogeneity. It should be remembered that the treatment is thermodynamic in nature, and attempts no description of the behavior of light in

* A notable example of the use of integral equation methods is the recent work of Moon who has dealt with problems of inter-reflections. P. Moon, J. Opt. Soc. Am. 30, 195 (1940) and J. Opt. Soc. Am. 32, 348 (1942).

[9] Channon, Renwick, and Storr, Proc. Roy. Soc. **A94**, 222 (1918).

[10] S. Q. Duntley, J. Opt. Soc. Am. **32**, 61 (1942).

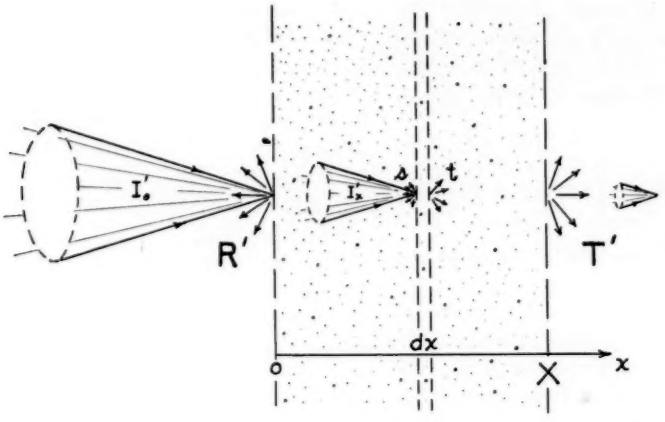

FIG. 3.

passing over the particles. For this reason, effects such as those explained by Rayleigh will appear as variations in the absorption and scattering coefficients.

The solution of the differential equations may be expressed in a variety of forms. Experience has shown the use of hyperbolic functions to be convenient. The following solutions have been patterned after those of Ryde.[11] From a parallel-sided slab of diffusing material having a thickness X, the total flux emergent in the transmission direction is:

$$\text{Total Emergent Flux (transmission direction)} = (Q'-1)\exp[-(\mu'X+B'X+F'X)]I_0' + \frac{Q'KX+P'\exp[-(\mu'X+B'X+F'X)]BX\sinh KX}{(\mu X+BX)\sinh KX+KX\cosh KX}I_0' + \frac{\mu X\sinh KX+KX\cosh KX-KX}{(\mu X+BX)\sinh KX+KX\cosh KX}E,$$

where: $K=[\mu(\mu+2B)]^{\frac{1}{2}}$;

$$P'=\frac{(\mu-\mu')B'+(B-B')(B'+F')}{(\mu'^2-\mu^2)+2\mu'(F'+B')-2\mu B+(F'+B')^2};\quad Q'=\frac{(\mu+\mu')F'+(B'+F')(B'+F')}{(\mu'^2-\mu^2)+2\mu'(F'+B')-2\mu B+(F'+B')^2}.$$

It will be noted that the first term of the solution represents light which has been transmitted unscattered, that the second term describes incident light that has experienced secondary scattering, and that the third term represents light produced within the medium. The corresponding solution for the total flux emergent from the medium in the reflection direction is:

$$\text{Total Emergent Flux (reflection direction)} = \frac{P'KX\exp[-(\mu'x+B'x+F'x)]+Q'BX\sinh KX}{(\mu X+BX)\sinh KX+KX\cosh KX}I_0'-P'I_0' + \frac{\mu X\sinh KX+KX\cosh KX-KX}{(\mu X+BX)\sinh KX+KX\cosh KX}E.$$

[11] J. W. Ryde, Proc. Roy. Soc. **131A**, 451 (1931).

The engineering use of solutions to Schuster-type equations has been discussed by numerous authors including Ryde,[12] Steele,[13] Judd,[14] Duncan,[15] Duntley,[10] and Saunderson.[16] Because of the very real industrial usefulness of turbid medium theory, it may be expected that further engineering developments based upon solutions of Schuster-type differential equations will appear as the art of photometry develops. Whether extensive engineering use will be made of the more general integral equation method of King only the future can tell. It stands today an unanswered mathematical challenge.

[12] J. W. Ryde, J. Soc. Glass Tech. **16**, 408 (1932).
[13] F. A. Steele, Paper Trade Journal **100**, No. 12 (1937).
[14] D. B. Judd, J. Research Nat. Bur. Stand. **19**, 287 (1937).
[15] D. R. Duncan, Proc. Phys. Soc. **52**, 380 (1940).
[16] J. L. Saunderson, J. Opt. Soc. Am. **32**, 727 (1942).

JOURNAL OF THE OPTICAL SOCIETY OF AMERICA VOLUME 33 NUMBER 5 MAY, 1943

Wave-Length Calibration of Spectrophotometers

J. A. VAN DEN AKKER
The Institute of Paper Chemistry, Appleton, Wisconsin

(Received March 15, 1943)

A STANDARDIZED didymium filter is very satisfactory for the calibration of the wave-length scale of a spectrophotometric instrument when the range of wave-lengths employed in the instrument is small.[1] When the range of wave-lengths is of the order of ten millimicrons or more, however, a didymium filter is useful only for the purpose of quickly checking the constancy of wave-length calibration, unless the spectral transmission has been determined on a standardized instrument similar to the one under calibration. Among the reasons for the failure of a didymium filter to furnish an accurate check against spectrum lines are the following: (a) The form of the spectral transmission curve is altered when the wave-length range is broadened.[1] (b) The wave-length read from a sharp maximum or minimum is often not the effective wave-length of interest (see later discussion). (c) In automatic, recording instruments, variations in instrumental sensitivity produce shifts in the positions of maxima and minima in the recorded curve; for example, a decrease in sensitivity will produce a shift towards longer wave-length in an instrument which continuously changes wave-length from smaller to larger values.

During the past three and a half years we have calibrated the wave-length scale of our General Electric recording spectrophotometer and determined the effective wave-lengths of various abridged spectrophotometers by means of a method based directly on theoretical considerations of "centroid wave-length." Since this method has proved to be very satisfactory, this note has been prepared with the hope that others might find the method useful when it is necessary to make a fairly direct comparison against spectrum lines.

The light emerging from the dispersing or filtering system of an instrument and falling upon the reflecting or transmitting substance under test has wave-lengths lying between λ_1 and λ_2. Let the spectral intensity distribution of the light source be E, the spectral transmission of the optical system (including filters, if any) be T_g, the spectral reflectance or transmission of the solid or filter under test be T, and the relative spectral sensitivity of the photo-cell or other receptor be S. The instrumental value for the reflectance or transmission should be

$$\bar{T}=\left[\int_{\lambda_1}^{\lambda_2} ET_gST d\lambda\right]\Big/\left[\int_{\lambda_1}^{\lambda_2} ET_gS d\lambda\right]. \quad (1)$$

It is clear that there can be no definite wave-length of *monochromatic* light for which the T

[1] Kasson S. Gibson and Harry J. Keegan, J. Opt. Soc. Am. **28**, 372 (1938).

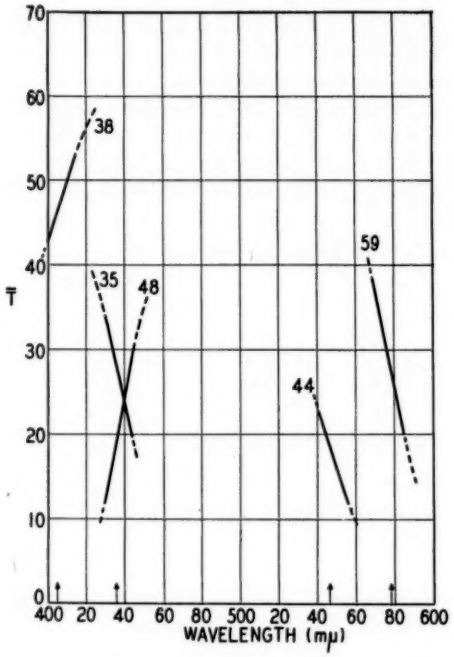

FIG. 1. Spectral transmission curves for five Wratten filters employed in determinations of effective wave-lengths with spectrum lines of mercury.

value will be the same as that given by Eq. (1) for all possible spectral reflectances or transmissions. However, in studies of the colorimetry of many substances, one deals with curves which do not have strong curvatures for the most part, so that the spectral reflectance or transmission is nearly linear over the range λ_1 to λ_2. A practical, definite meaning to the term *effective wave-length* obtains when $T=a+b\lambda$. On substituting this expression in Eq. (1) we obtain

$$\bar{T}=a+b\left[\int_{\lambda_1}^{\lambda_2} ET_\varrho S\lambda d\lambda\right]\Big/\left[\int_{\lambda_1}^{\lambda_2} ET_\varrho S d\lambda\right]. \quad (2)$$

There is then a definite wave-length,

$$\lambda_e=\left[\int_{\lambda_1}^{\lambda_2} ET_\varrho S\lambda d\lambda\right]\Big/\left[\int_{\lambda_1}^{\lambda_2} ET_\varrho S d\lambda\right], \quad (3)$$

which, by identification with the assumed linear equation, is seen to be the wave-length of monochromatic light for which the reflectance or transmission is equal to that obtained with the heterogeneous light. The slope of the assumed linear relationship may vary from large negative to large positive values, but the effective wave-length λ_e will remain constant. Error develops only when the curvature becomes strong, as at a sharp knee, peak, or valley. The "centroid wave-length" λ_e is the only weighted average which has practical significance and depends upon only instrumental factors. Before proceeding to the discussion of the utilization of Eq. (2) in wave-length calibration, it should be pointed out that the effective wave-length is not independent of the slopes of the curves for E, T_ϱ, and S, and hence it does not lie midway between λ_1 and λ_2.

The foregoing theory furnishes a direct method for evaluating the effective wave-length of a spectrophotometer for any desired setting of its wave-length scale. We may choose an optical filter having linear spectral transmission over the range λ_1 to λ_2 and measure the transmission of this filter with the instrument under calibration, at the desired wave-length setting. The spectral transmission for the wave-length range of interest is then determined with spectrum light, and the effective wave-length taken as that for which the monochromatic transmission is the same as the transmission observed with the spectrophotometer under calibration.

We have found it more satisfactory to reverse the above procedure, starting with a given spectrum line and finding the wave-length setting of the instrument for which the instrumental transmission is the same as the monochromatic transmission. The difficulties attending the determination of spectral transmission with a spectrograph and photometer and error due to photometric imperfections of either or both instruments are eliminated by operating the spectrophotometer with spectrum light. In calibrating the General Electric recording spectrophotometer the incan-

TABLE I.

Known wave-length mμ	Wratten filter No.	Transmission %	Indicated wave-length mμ	Correction to be added mμ
404.7	38	45.7	404.9	−0.2
435.7	48	17.7	435.1	+0.6
435.7	35	29.3	434.9	+0.8
546.1	44	18.5	546.4	−0.3
578.0	59	28.1	578.1	−0.1

descent lamp is removed, a mirror inclined at 45° is placed at a suitable elevation in the lamp house, and a d.c. mercury arc and condensing lens are arranged vertically above the lamp house. A small virtual image of the arc is formed by the lens and mirror at the point normally occupied by the filament of the incandescent lamp, and the system is adjusted to illuminate the objective lens of the monochromator in a manner roughly simulating the normal illumination. The instrument is set into operation with spectrum light. Filters appropriate for the more intense lines of the mercury spectrum are chosen, and their transmissions determined with spectrum light isolated by means of the double monochromator of the instrument. Following careful determination of the transmissions of the filters, the spectrophotometer is placed in normal operation with the incandescent lamp, and each filter is placed in the "sample beam" in exactly the orientation used during the operation with spectrum light. The wave-length cams are manually adjusted to obtain the same transmissions as observed with spectrum light, and the wave-length scale is read.

Data obtained in the most recent calibration illustrate the method as used with spectrum lines of mercury. The results are given in Table I. With the exception of the wave-length of the single line at 546.1 mμ, the data of column one are the weighted averages of wave-lengths of lines making up groups.

As shown in Fig. 1, filters are chosen which have large slopes in the ranges of interest. A typical value for the slope is 1 percent (transmission unit) per millimicron, so that an uncertainty of 0.1 percent in the photometric reading produces a wave-length error of about 0.1 mμ. The independence of a determination from algebraic sign of the slope is illustrated by the results obtained in the last three calibrations, in which Wratten filters 35 and 48 (having slopes of opposite sign) were used for obtaining the wave-length scale reading for the effective wave-length at 435.7 mμ. The differences between the scale readings for these two filters were 0.0, +0.1, and −0.2 mμ, an average difference of only −0.03 mμ.

In certain instruments the addition of a filter will modify the optical path length and thereby change the relative distribution of light over an aperture, which change, in turn, might subject the transmission value to appreciable error. In this case the transmission should be measured relative to that of a filter of similar thickness and index of refraction, but having essentially constant spectral transmission. This may be illustrated with the determination of the effective wave-length of a photoelectric instrument which employs a filter for the isolation of a portion of the spectrum. Due to the breadth of the wave-length range transmitted by this filter, it may be desirable to employ a liquid filter, the spectral transmittance of which is linear over the wave-length range. The colored solution and clear solvent are contained in a pair of nearly identical cells, which are preferably thin. The transmittance is then determined in the usual manner, placing the two cells alternately in the same position in the optical system of the instrument. Immediately following this measurement, the two cells may be placed in a spectrophotometer and the effective wave-length determined by manually adjusting the wave-length to obtain the same transmittance.[2]

[2] It may be necessary to make corrections for photometric errors, and for greater than normal path length through the filter, in the event that the beam of light is appreciably convergent or divergent.

A Metric for Colorspace*

PARRY MOON, *Massachusetts Institute of Technology, Cambridge, Massachusetts*

AND

DOMINA EBERLE SPENCER, *The American University, Washington, D. C.*

1. INTRODUCTION

THE familiar C.I.E. system of color specification is based on experiments with exact color matches. Its geometric representation is an affine space in which, as in any affine space, angles and distances cannot in general be compared. It is natural for the colorimetrist to inquire if additional information can be obtained by introducing a metric into the affine colorspace. Helmholtz[1] was the first to take such a step, and he identified the metric with minimum perceptible color difference. If a successful metric can be established, it will widen the scope of the C.I.E. colorspace by giving a geometric representation to all available information on color discrimination. Considerable previous effort has been devoted to the subject, without, however, leading to any completely satisfactory solution.

The present paper develops a metric for colorspace. The method employs non-linear transformations in place of the linear transformations ordinarily used; and the conclusions are based on experimental results rather than on speculations. In presenting this material, we first give an elementary outline of the basic mathematical ideas. Such an outline would be superfluous for mathematicians but may prove helpful to colorimetrists. A metric is then introduced in a plane of constant helios,[2,3] after which it is extended to the color 3 space.

The Riemannian metric is written

$$(ds)^2=g_{ij}dx^i dx^j, \quad (i, j=1, 2, 3) \qquad (1)$$

where dx^i and dx^j are elementary distances along any three coordinate axes. The metric coefficients g_{ij} may be constants or they may be arbitrary functions of the coordinates x^1, x^2, x^3. Equation (1) may be regarded as the definition of a quantity ds by which distances are determined between pairs of points in the coordinate space.

If the coordinate surfaces are orthogonal, Eq. (1) becomes

$$(ds)^2=g_{11}(dx^1)^2+g_{22}(dx^2)^2+g_{33}(dx^3)^2. \qquad (2)$$

For the special case where the metric coefficients are all unity, the Euclidean metric is obtained:

$$(ds)^2=(dx^1)^2+(dx^2)^2+(dx^3)^2. \qquad (3)$$

When the Euclidean metric is introduced into an affine space, the space becomes the familiar space of elementary geometry.

The ordinary affine colorspace can be changed to a metric space by introducing any metric that the investigator desires. There is nothing in the C.I.E. data to indicate what metric is to be used, nor do philosophical speculations lead to anything of value. *The metric coefficients must be obtained by consideration of additional experimental data.* Available data are of two kinds: color discrimination taken at constant helios, and contrast sensitivity obtained at constant chromaticity.

Consider a region of space about a given point P, the region being so small that the metric coefficients can be considered as constants. We inquire as to the shape of the surface $\Delta s=1$, which lies in the foregoing restricted region of space. The equation of the surface is, according to Eq. (1),

$$\frac{(\Delta x^1)^2}{(1/g_{11})}+\frac{(\Delta x^2)^2}{(1/g_{22})}+\frac{(\Delta x^3)^2}{(1/g_{33})}+\frac{\Delta x^1\cdot\Delta x^2}{(1/g_{12})}+\frac{\Delta x^1\cdot\Delta x^3}{(1/g_{13})}+\frac{\Delta x^2\cdot\Delta x^3}{(1/g_{23})}=1, \qquad (4)$$

where the g's are constants. But this is the equation of an *ellipsoid.*** The principal axes of the

* Based on a paper presented by one of the authors at the annual meeting of the Optical Society of America, New York, October 31, 1942.

[1] H. v. Helmholtz, Berlin Akad. Sci. 1071 (1891). *Handbuch der physiologischen Optik* (Leipzig, 1896), second edition.

[2] Parry Moon, J. Opt. Soc. Am. **32**, 348 (1942).

[3] D. E. Spencer, J. Opt. Soc. Am. **33**, 10 (1943).

** Equation (4) represents a quartic surface. However, in this application it must be a quartic surface that remains finite and hence an ellipsoid.

ellipsoid are generally not in the directions of the coordinate axes. But if the coordinate axes are axes of symmetry of the ellipsoid, Eq. (4) becomes

$$\frac{(\Delta x^1)^2}{(1/g_{11})}+\frac{(\Delta x^2)^2}{(1/g_{22})}+\frac{(\Delta x^3)^2}{(1/g_{33})}=1. \qquad (5)$$

$1/g_{11}$, $1/g_{22}$, and $1/g_{33}$ are the lengths of the semi-axes of the ellipsoid if the coordinate axes are orthogonal with respect to this metric.

Thus by rotation of the coordinate axes until they are orthogonal and are parallel to the principal axes of the ellipsoid, any particular ellipsoid can be represented by the foregoing simple equation. The surface of colors that are just perceptibly different from a given color P is then an ellipsoid having its principal axes in the direction of the coordinate axes and its center at P. The three axes of the ellipsoid are generally different because g_{11}, g_{22}, and g_{33} are not the same.

Any colorspace can be made locally Euclidean. But the metric coefficients will generally be different at two distinct points P and Q. Thus if the ellipsoid at P is transformed into a sphere, the one at Q will ordinarily remain an ellipsoid. In the special case in which a single transformation of variables eliminates the cross products for all points in space, Eq. (4) becomes

$$g_{11}(x^1, x^2, x^3)\cdot(\Delta x^1)^2+g_{22}(x^1, x^2, x^3)\cdot(\Delta x^2)^2 +g_{33}(x^1, x^2, x^3)\cdot(\Delta x^3)^2=1. \qquad (6)$$

A Euclidean metric is possible for the whole space if the following new variables can be introduced:

$$\Delta\xi^i=(g_{ii}(x^1, x^2, x^3))^{\frac{1}{2}}\cdot\Delta x^i, \quad (i=1, 2, 3). \qquad (7)$$

In general, however, no such simplicity obtains and no Euclidean metric is possible.

2. A METRIC IN A PLANE OF CONSTANT HELIOS

One method of introducing a metric into colorspace is to assume a Euclidean metric and to find what linear transformation of the C.I.E. space will give a reasonable approximation to the experimental data on color discrimination. This method is obviously doomed to failure in the 3 space since it gives no approximation to the well-established effect of helios variation. In the 2 space, however, it can be put in reasonably good agreement with experiment. Judd[4] was the first to use a projective transformation of the C.I.E. chromaticity diagram in an attempt to find a metric, and the resulting Maxwell triangle was found to give fairly good agreement with most experimental results on color discrimination. Other projective transformations giving similar results have been originated by MacAdam,[5] Breckenridge and Schaub,[6] Sinden,[7] and Adams.[8] The present paper differs from its predecessors in using *non-linear* transformations, and it will be shown that the resulting 2 space has advantages over the others.

Numerous researches have been conducted on the minimum perceptible color variation at constant helios, or on related quantities. The most recent investigation is that of MacAdam[9] who kept the helios of the test spots at a value of 150 blondels and who employed a surround having half this helios.[2] Illuminant C was used in lighting the surround. Twenty-five points were taken in the color 2 space. For each point, color matches were made along a number of lines in the chromaticity diagram; and for each line the standard deviation of the results was computed. It was found that the standard deviation determined an ellipse about the chosen point.

When the MacAdam ellipses are plotted in the C.I.E. chromaticity diagram[9] (Fig. 1), they are found to be of different sizes and orientations so that no Euclidean metric can be employed in this diagram. To obtain values of the metric coefficients g_{11}, g_{13}, and g_{33} of Eq. (1), we replotted the ellipses in the plane of constant helios, $Y=150$, using the equations,

$$X=150x/y, \qquad Z=150(1-x-y)/y. \qquad (8)$$

The surprising result was that the major axes of the ellipses became essentially parallel. In fact, the MacAdam data can be fitted by a set of ellipses with major axes having the slope in the XZ plane of $+4.32$. These ellipses are shown in

[4] D. B. Judd, J. Opt. Soc. Am. **25**, 24 (1935); J. Research Nat. Bur. Stand. **14**, 41 (1935).
[5] D. L. MacAdam, J. Opt. Soc. Am. **27**, 294 (1937).
[6] Breckenridge and Schaub, J. Opt. Soc. Am. **29**, 370 (1939).
[7] R. H. Sinden, J. Opt. Soc. Am. **27**, 124 (1937); **28**, 339 (1938).
[8] E. Q. Adams, J. Opt. Soc. Am. **32**, 168 (1942).
[9] D. L. MacAdam, J. Opt. Soc. Am. **32**, 247 (1942).

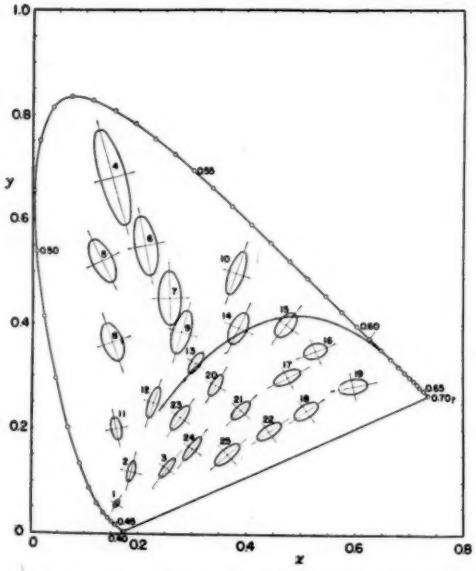

FIG. 1. The MacAdam ellipses in the C.I.E. chromaticity diagram. The dimensions of the ellipses are ten times the standard deviations.

Fig. 2, where the numbering is the same as in Fig. 1. The data are given in Table I.

The relation between the diagrams of Fig. 1 and Fig. 2 is illustrated in Fig. 3. The locus of colors of a given chromaticity is represented in the 3 space by a line through the origin. This line intersects the unit plane at a point (x, y, z), where the three coordinates are not independent but are related by the equation of the unit plane:

$$x+y+z=1. \tag{9}$$

The projection of the unit-plane diagram onto the XZ plane gives the familiar C.I.E. diagram. A plane of constant helios is any plane where $Y=$const. Evidently the projection of the MacAdam ellipses onto a plane of constant helios reorients them and changes their ellipticity, the part of the diagram representing blues and violets being stretched out greatly in the Z direction.

The Euclidean metric is introduced after performing a rotation of the coordinate system so that the new axes are parallel to the axes of the ellipses. The new axes obtained in this way are called U and V (Fig. 2) and are specified by

$$\begin{aligned} U&=0.974X-0.226Z, \\ V&=0.226X+0.974Z. \end{aligned} \tag{10}$$

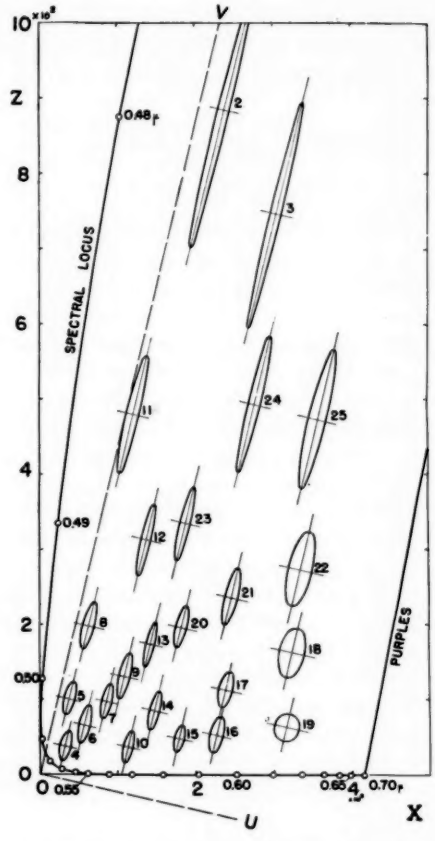

FIG. 2. The MacAdam ellipses transferred to a plane of constant helios ($H=Y=150$ blondels).

The space is made Euclidean by suitable transformations of U and V. Figure 2 indicates that the length of the major axis depends only on V, while the minor axis depends only on U. Thus the length of the major semi-axis may be plotted against V and the minor semi-axis against U, as shown in Figs. 4 and 5.

Analytical expressions must now be found to represent the two sets of points, or

$$\begin{aligned} &\text{Minor semi-axis of ellipse}=f_1(U), \\ &\text{Major semi-axis of ellipse}=f_3(V). \end{aligned}$$

For a Euclidean space, the ellipses must transform into circles, all with the same radius; and if Δs is to be unity for the standard deviation, the radius of all circles must be unity. In the plane

of constant helios, therefore, the metric is

$$(ds)^2=(dU/f_1(U))^2+(dV/f_3(V))^2. \quad (11)$$

The UV plane is transformed into a plane in which the metric is Euclidean,

$$(ds)^2=(d\xi^1)^2+(d\xi^3)^2, \quad (12)$$

where

$$d\xi^1=dU/f_1(U), \quad d\xi^3=dV/f_3(V). \quad (13)$$

Thus the equations for the transformations are

$$\xi^1=\int \frac{dU}{f_1(U)}+C^1, \quad \xi^3=\int \frac{dV}{f_3(V)}+C^3, \quad (14)$$

where C^1 and C^3 are constants of integration.

Evidently neither set of data (Fig. 4 or 5) can be represented by a linear function, so no projective transformation[5] of the C.I.E. chromaticity diagram will adequately represent the experimental evidence. The data of Fig. 4, however, are fitted very well by the parabola:

$$f_1(U)=0.60+0.268\left(\frac{U}{100}-1\right)^2. \quad (15)$$

In fact, no other satisfactory expression for $f_1(U)$ has been found.

For the data of Fig. 5, however, the MacAdam ellipses extend to only $V=2100$ while the extreme violet of the spectral locus is at $V=26{,}000$. No data are available in the intervening region; so a number of equations can be used for $f_3(V)$ which will fit the data equally well but which will behave differently at large values of V. The first equation tried was

$$f_3(V)=2.00+0.220(V/100)^2, \quad (16)$$

which is in excellent agreement with the data except for Ellipses 1 and 2 (Table I). The new

TABLE I. Ellipses in a plane of constant helios ($H=150$ blondels).

No.	Fig.*	Center				Major semi-axis	Minor semi-axis
		X	Z	V	U		
1	23	420	2058	2100	−54	31.0	1.25
2	24	238	884	915	+34	19.7	0.70
3	25	304	746	796	128	15.6	0.70
4	26	33.1	37.5	44.0	23.7	1.98	0.76
5	27	37.7	100	105.9	14.2	2.23	0.79
6	28	57.9	65.0	76.3	41.8	2.63	0.70
7	29	86.0	97.2	114.1	61.7	2.37	0.68
8	30	62.5	198	207.3	16.1	3.32	0.82
9	31	191	130	170	156	3.10	0.68
10	32	114	36.7	61.5	103	2.15	0.65
11	33	120	480	494	8.8	8.00	0.80
12	34	137	313	336	63.0	5.00	0.65
13	35	142	173	200	99.2	3.20	0.58
14	36	147	84.7	115.7	124.1	2.65	0.60
15	37	178	48.5	87.3	162.3	1.85	0.70
16	38	226	52.7	102.3	208	2.50	0.90
17	39	238	112.5	163.2	207	2.38	0.90
18	40	324	162	231	279	3.30	1.50
19	41	316	64.2	133.8	293	1.84	1.60
20	42	182	196	232	133	2.93	0.68
21	43	246	236	286	187	3.85	0.80
22	44	335	274	342	264	5.00	1.45
23	45	187	335	368	106	5.00	0.65
24	46	276	494	543	157	9.20	0.70
25	47	358	473	541	241	9.50	1.15

Average slope of major axes = 4.32.
* Figure number from MacAdam's paper.

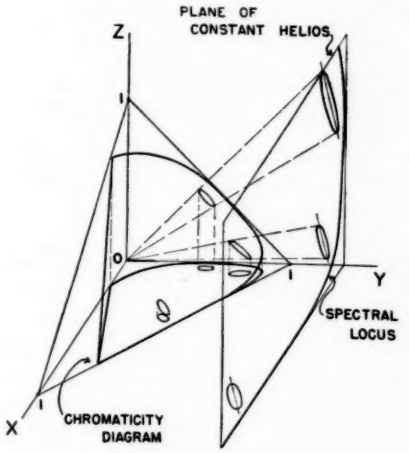

FIG. 3. Three-dimensional representation showing the relation between the chromaticity diagram and a plane of constant helios.

coordinates, according to Eq. (14), are

$$\xi^1=250\tan^{-1}\left[0.668\left(\frac{U}{100}-1\right)\right]+C^1,$$
$$\xi^3=150.8\tan^{-1}[0.331(V/100)]+C^3. \quad (17)$$

The spectral locus shows a point of inflection in the ξ diagram and is found to be concave from about 0.40 to 0.50μ. This characteristic is rather startling, since in previous diagrams the locus has always been convex.[4] In fact, it is easy to prove that the convexity of the spectral locus is an affine invariant. Though there appears to be no *a priori* reason why the same should be true in the ξ diagram, we thought it advisable to investigate the possibility of a convex locus. Accordingly, various transformations were considered,

among which may be mentioned:

$$f_3(V)=17.3-16.4\tanh\left[\frac{2(850-V)}{1000}\right], \tag{18}$$

$$f_3(V)=\frac{1.50+0.346(V/100)^2}{1+0.0090(V/100)^2}, \tag{19}$$

$$f_3(V)=2.20+\frac{V}{100}[2.0-2.6e^{-0.26V/100}], \tag{20}$$

$$f_3(V)=\frac{2.20+0.540(V/100)^2}{1+0.180(V/100)}, \tag{21}$$

$$f_3(V)=\frac{2.20+0.540(V/100)^2}{1+0.180(V/100)+0.010(V/100)^2}. \tag{22}$$

These equations are in equally good agreement with the MacAdam ellipses but result in different behavior of the spectral locus in the ξ diagram from 0.40 to 0.50μ.

Equations (18) and (19) move the violet end of the spectrum to very high values of ξ^3, which is not in agreement with data on the number of steps from white to the spectral locus.[10] Some of the other equations are inconvenient. The best one appears to be Eq. (21). It still gives a slight concavity of the locus, but it agrees with all the MacAdam ellipses (including Nos. 1 and 2) and it appears to be in reasonable agreement with all other pertinent data. Equation (22) may also be used, and the coefficient of the final term in the denominator may be altered through a considerable range without change in the other constants. Until more complete data at short wave-lengths are available, however, this additional refinement appears to be unnecessary. From a study of the various transformations, we have reached the conclusion that a concavity of the spectral locus cannot be avoided in the ξ diagram except by modification of either the MacAdam data or the C.I.E. trichromatic data.

On the basis of available data, therefore, we recommend the use of Eq. (21). The metric coefficients are:

$$g_{11}=\left[0.60+0.268\left(\frac{U}{100}-1\right)^2\right]^{-2},$$
$$g_{13}=0, \tag{23}$$
$$g_{33}=\left[\frac{1+0.180(V/100)}{2.20+0.540(V/100)^2}\right]^2.$$

The transformations to the ξ diagram are:

$$\xi^1=250\tan^{-1}\left[0.668\left(\frac{U}{100}-1\right)\right]+C^1,$$
$$\xi^3=91.8\tan^{-1}\left(0.495\frac{V}{100}\right)$$
$$+16.67\ln\left[2.2+0.54\left(\frac{V}{100}\right)\right]+C^3. \tag{24}$$

The constants C^1 and C^3 are entirely arbitrary. The simplest transformation is obtained by mak-

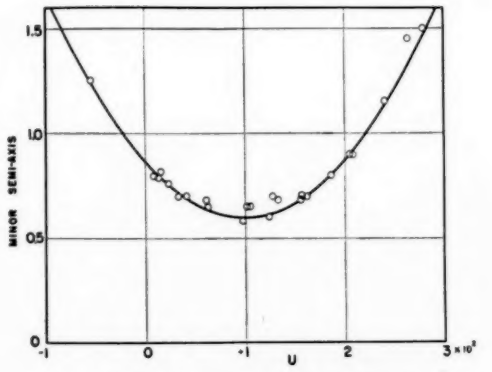

FIG. 4. Minor semi-axes of the MacAdam ellipses in the plane $Y=150$.

[10] Martin, Warburton, and Morgan, Med. Res. Council Report, London (1933).

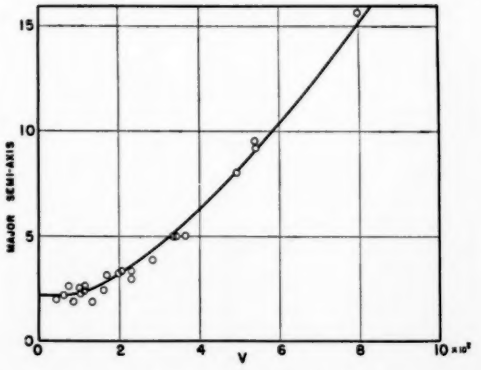

FIG. 5. Major semi-axes of the MacAdam ellipses in the plane $Y=150$.

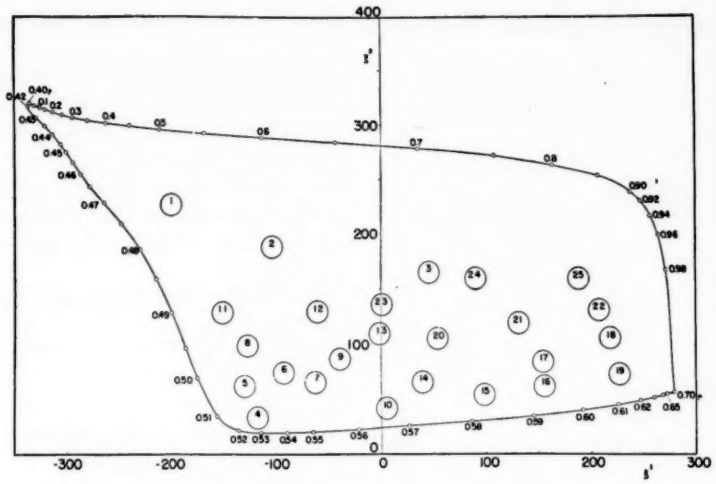

FIG. 6. MacAdam ellipses transferred to the $\xi^1\xi^3$ diagram. All the ellipses become circles of equal size. The numbering agrees with that of Fig. 1.

ing them both zero, as will be done in this paper. There is a slight advantage for some purposes in placing the center of coordinates at an achromatic point, in which case the different quadrants contain related colors much as in the Breckenridge diagram.[6]

Use of Eq. (24) results in the peculiar prow-shaped diagram of Fig. 6. The curve of saturated purples was obtained by taking 10 equally-spaced points between the extremes of the spectral locus in the C.I.E. chromaticity diagram. The result is not a straight line because of the non-linear transformation of Eq. (24). The transformed MacAdam ellipses are now circles, all with unit radius. The dimensions of these circles in Fig. 6 are made ten times their true values, as was done with the original ellipses (Fig. 1). The numerical designation of the MacAdam circles also agrees with that of Fig. 1.

Typical transformed ellipses are shown in Figs. 7, 8, 9, and 10. The dots are the MacAdam experimental points, transformed by means of Eq. (24). These points are in reasonably good agreement with the heavy circles having unit radius. Light circles having radii which differ by ± 30 percent from the heavy circles indicate the approximate limits of scatter of the experimental data. In some cases the points seem to indicate an ellipticity, but it is doubtful if this appearance has any validity. Note that the wide variations in size and shape, shown in Figs. 1 and 2, have disappeared. The other MacAdam circles are not shown, in order to save space. However, within the limits of experimental error, all of the data are representable by unit circles.

3. A METRIC IN 3 SPACE

Helmholtz[1] based his metric on experimental results in 1 space (variation of helios only), which gave

$$(ds)^2=(dH/[a+bH])^2.$$

He considered as a "probable hypothesis" that the extension to 3 space would give

$$(ds)^2=\left(\frac{dx^1}{a^1+x^1}\right)^2+\left(\frac{dx^2}{a^2+x^2}\right)^2+\left(\frac{dx^3}{a^3+x^3}\right)^2, \quad (25)$$

where x^i are the amounts of the "physiologischen Urfarben" and a^i are constants. This provides a Euclidean metric in the variables ξ^i, where

$$\xi^i=\ln\,(a^i+x^i)+C^i. \quad (26)$$

Because of the scarcity of experimental data, there was little that Helmholtz could do except make a reasonable guess such as Eq. (25). His metric, however, did not agree with the König

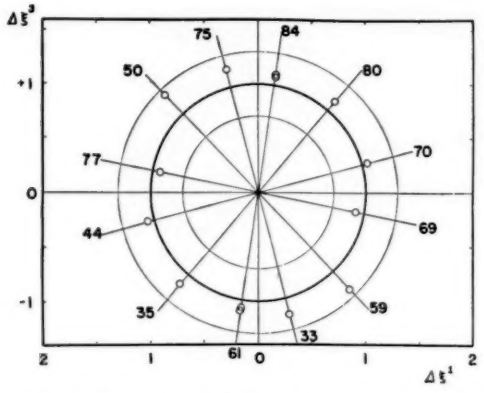

FIG. 7. MacAdam data for his Fig. 31 (white) transformed into ξ space.

data then available, nor does it fit more recent experimental results.

Schrödinger chose the metric,

$$(ds)^2=\frac{1}{x^1+x^2+x^3}\left[\frac{(dx^1)^2}{x^1}+\frac{(dx^2)^2}{x^2}+\frac{(dx^3)^2}{x^3}\right]. \quad (27)$$

His choice was largely arbitrary, though governed to some extent by his peculiar ideas of "equibrightness." Comparison with experiment showed that[11] "Die Konstanz von ds ist sehr schlecht erfüllt, ungefähr ebenso schlecht wie bei Helmholtz." Interesting theoretical work has been done on the color metric by Silberstein.[12] Bouma[13] has also written on the subject.

The metric considered in Section 2 is in a plane of constant helios. It will now be extended to 3 space by use of data on minimum perceptible helios variation at constant chromaticity. Such data have been obtained by König and Brodhun[14] and by many other investigators, and all the data are fitted by an equation of the form,

$$(\Delta Y)_{\min}=A+BY, \quad (28)$$

where B, the so-called "Fechner fraction," is approximately 0.015. If the standard deviation is employed, instead of the minimum perceptible, the value becomes approximately 0.005.

Most of these experiments have been made with unmodified light from incandescent lamps; but the tests have shown that essentially the same curve is obtained with homogeneous radiation, irrespective of the wave-length in the visible region.[14] This means that the standard deviation for any line of constant quality is given by Eq. (28).

But for any line of constant quality,

$$dU/U=dV/V=dY/Y. \quad (29)$$

For such a line,

$$(ds)_q^2=[dY/f_2(Y)]^2, \quad (30)$$

which expresses the fact that the standard deviation is a function of Y only, for any line passing through the origin of colorspace. Take the U, V, and Y axes orthogonal. Then, as indicated in Section 1, the metric coefficients g_{12} and g_{23} are zero when the ellipses, $\Delta s=$const., have their principal axes in the directions of the coordinates. Thus the metric for the general 3-dimensional case is

$$(ds)^2=g_{11}(dU)^2+g_{22}(dY)^2+g_{33}(dV)^2. \quad (31)$$

From Eq. (29), for the special case of constant quality,

$$(ds)_q^2=\left(\frac{dY}{Y}\right)^2[g_{11}\cdot(U)^2 +g_{22}\cdot(Y)^2+g_{33}\cdot(V)^2] \quad (32)$$

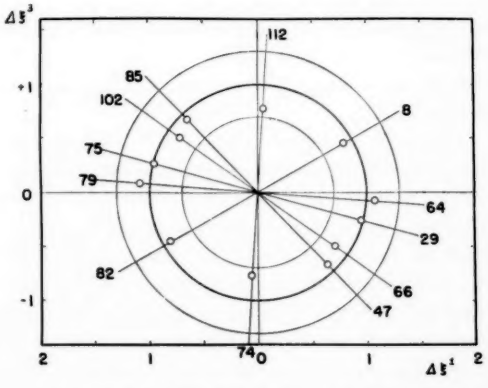

FIG. 8. MacAdam Fig. 33 (blue) in ξ space.

[11] E. Schrödinger, Ann. d. Physik **63**, 481 (1920).
[12] L. Silberstein, J. Opt. Soc. Am. **28**, 63 (1938); **32**, 552 (1942).
[13] P. J. Bouma, Amsterdam Acad. Sci. **38**, 35, 148, 258 (1935).
[14] König and Brodhun, *Gesammelte Abh.* (Leipzig, 1903), p. 116. Stiles and Crawford, Proc. Roy. Soc. London, **116B**, 55 (1934); Proc. Roy. Soc. London, **113B**, 496 (1933). J. Steinhardt, J. Gen. Physiol. **20**, 185 (1936).

and by use of Eq. (30)

$$g_{22}=\frac{1}{(Y)^2}\left[\left(\frac{Y}{f_2(Y)}\right)^2-g_{11}\cdot(U)^2-g_{33}\cdot(V)^2\right]. \quad (33)$$

As shown in the first part of this section, the experimental results give

$$f_2(Y)=A+BY.$$

But except at values of helios below 10 blondels, the first term can be omitted. It seems hardly necessary at present to attempt the representation of color discrimination at lower values of helios, since the whole C.I.E. system is based on data obtained at higher values of helios and is inapplicable at low values. Thus $f_2(Y)$ will be taken as $0.005Y$, and Eq. (33) becomes

$$g_{22}=\frac{1}{(Y)^2}[(200)^2-g_{11}\cdot(U)^2-g_{33}\cdot(V)^2]. \quad (33a)$$

It now becomes necessary to express g_{11} and g_{33} in a more general form than was employed in

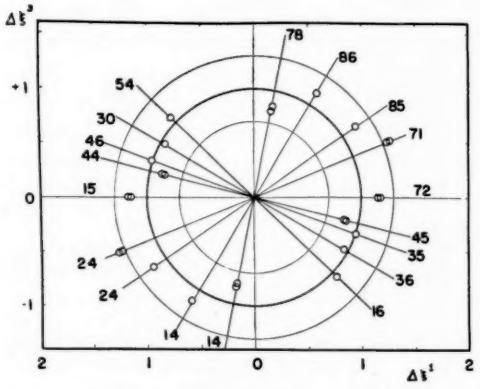

FIG. 9. MacAdam Fig. 26 (green) in ξ space.

Section 2. These coefficients were obtained for the special case of the plane $Y=150$. To make them of general value, in accordance with the simplified form of $f_2(Y)$, we replace the previous variables U and V by $U(150/Y)$ and $V(150/Y)$. Evidently if $Y=150$, everything remains in accordance with the experimental results of Section 2. Along a given line of constant chromaticity, however, $U/Y=V/Y=\text{const}$. Therefore, for this line ξ^1 and ξ^3 are constants, irrespective of the value of Y. Equations (23) and (33a) now become

$$g_{11}=\left[0.60+0.268\left(\frac{3U}{2Y}-1\right)^2\right]^{-2},$$

$$g_{33}=\left[\frac{1+0.180(3V/2Y)}{2.20+0.540(3V/2Y)^2}\right]^2,$$

$$g_{22}=\left(\frac{200}{Y}\right)^2-\frac{(U/Y)^2}{[0.60+0.268(3U/2Y-1)^2]^2} \quad (34)$$

$$-\left[\frac{1+0.180(3V/2Y)}{2.20+0.540(3V/2Y)^2}\right]^2(V/Y)^2.$$

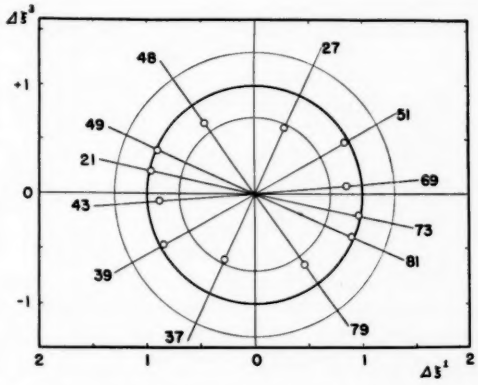

FIG. 10. MacAdam Fig. 41 (red) in ξ space.

These are the general metric coefficients applying in Eq. (31) to the 3-dimensional colorspace. The final coordinate transformations are now written

$$\xi^1=250.0\tan^{-1}\left[0.668\left(\frac{3U}{2Y}-1\right)\right],$$

$$\xi^3=91.80\tan^{-1}\left[0.495\frac{3V}{2Y}\right]$$

$$+16.67\ln\left[2.20+0.540\left(\frac{3V}{2Y}\right)^2\right], \quad (35)$$

$$\xi^2=\left[(200)^2-\frac{(U)^2}{[0.60+0.268(3U/2Y-1)^2]^2}\right.$$

$$\left.-\left[\frac{1+0.180(3V/2Y)}{2.20+0.540(3V/2Y)^2}\right]^2(V)^2\right]^{\frac{1}{2}}\ln Y.$$

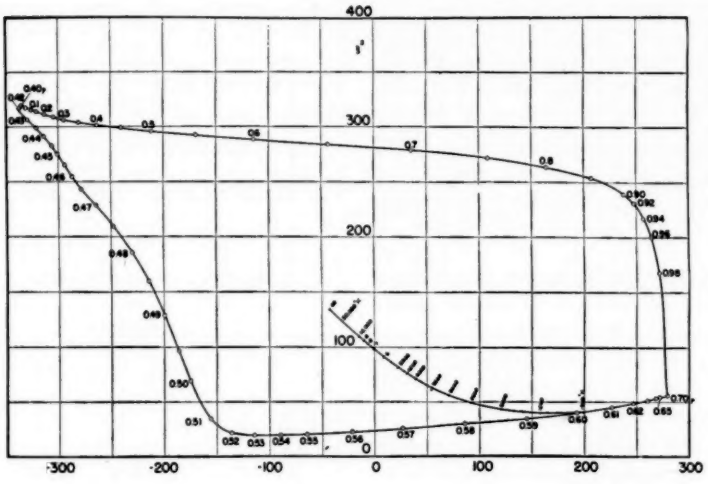

FIG. 11. The $\xi^1\xi^3$ diagram showing spectral locus, line of saturated purples, and Planckian locus.

Here $Y=H=$helios, expressed in blondels, and U and V are obtained from Eq. (10).

Equation (35) shows that the $\xi^1\xi^3$ diagram is exactly the same for any value of helios. Thus whenever interest is in chromaticity only and the helios is constant, the $\xi^1\xi^3$ diagram plays a role similar to that of the familiar C.I.E. chromaticity diagram. The ξ diagram is shown again in Fig. 11 with the Planckian locus included. All information on color discrimination at constant helios, such as minimum perceptible wave-length difference along the spectral locus, can be obtained directly from the diagram. If helios variation is also encountered, the 3 space is used (Fig. 12). The surfaces $\Delta s=1$ are spheres of the same size throughout the ξ space, and the spectral locus is a cylinder. Distances between points have the same significance as in the 2 space.

4. SUMMARY

The paper develops a new metric for colorspace. It is found that, within the limits of experimental error, data on color discrimination can be fitted by the Euclidean metric,

$$(ds)^2=(d\xi')^2+(d\xi^2)^2+(d\xi^3)^2,$$

where ξ^1, ξ^2, and ξ^3 are new coordinates which are related to the C.I.E. coordinates by elementary (though non-linear) functional transformations. The familiar C.I.E. affine colorspace is transformed into a three-dimensional ξ space in which minimum perceptible color differences are represented by small spheres of the same size throughout the space. Geodesics are straight lines, and all the other properties of elementary Euclidean geometry apply directly in this new colorspace.

Planes of constant helios in the C.I.E. space transform into planes in the ξ space. All of these $\xi^1\xi^3$ diagrams are identical and give a Euclidean representation of the C.I.E. chromaticity diagram. It can be shown that the new 2 space is in

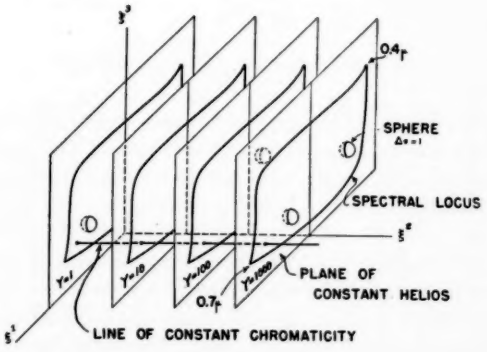

FIG. 12. The three-dimensional ξ space.

better accord with experimental data than has been obtained with the projective transformations, which were developed previously.[5]

The new ξ space has important applications in colorimetry and gives for the first time a mathematical method of comparing colors which differ both in quality and quantity. It should be emphasized, however, that the new system does not in any way replace the C.I.E. system but only supplements it. Colors are first specified in terms of X, Y, and Z; and these values can then be transformed into ξ^1, ξ^2, and ξ^3. The ξ space has many advantages, but these advantages have been obtainable only by giving up the simple geometric representation of addition. The addition of two colors cannot be obtained vectorially in ξ space, and straight lines in the C.I.E. space are transformed into curves in the new space.

Book Review

Prism and Lens Making. F. TWYMAN. Pp. 178. Adam Hilger, Ltd., London, 1942.

In the field of optical manufacture, in which there is such a dearth of literature, an addition such as this is welcome. As stated by the author, the purpose of the book is to describe the methods and machines used in the production of precision optical parts, with particular reference to those in use in the shops of Adam Hilger, Limited. In these days of free interchange of information and methods which were formerly scrupulously guarded as trade secrets, the optical industry has been somewhat remiss. Any such attempt as this, therefore, to break down old-fashioned reticence is strongly to be commended.

The book opens with a review of the historical development of lens-making, the early Greek and Roman references to burning glasses, the thirteenth century development of spectacles, and the somewhat later introduction of the telescope and other familiar instruments. The reader will doubtless be struck by the fact that the art of making lenses has changed but little in fundamental methods from those used by the very earliest workers. Considerable discussion is given on the highly controversial subject of the nature of the grinding and polishing operations.

Of particular interest in the chapter on tools and materials, is the exposition of abrasive grain classification as worked out at the Hilger plant. This is an attempt to change from an arbitrary numbering of grain sizes to a logical system based directly on particle size.

The author takes up the various steps in the production of lenses and prisms in quantity. The centering and edging of lenses is treated in a separate chapter, together with the cementing of optical parts. Another chapter is devoted to the difficult subject of prism manufacture.

The section describing the testing of optical components should be of interest not only to the manufacturing optician but to every user of optical parts. The usual techniques are described as well as the use of special apparatus developed at the Hilger plant, among them the Hilger lens and prism interferometer, a precision instrument of wide application. The testing of optical glass for veins, imperfect annealing, and lack of homogeneity is given extended treatment.

An appendix is included giving data on light sources and the coating of glass to produce reflecting and non-reflecting surfaces. Also to be found here is a valuable section on the annealing of viscous materials such as pitch, cement, and optical glass. A useful glossary of English, French, and American optical terms is given.

More detailed descriptions and sketches of some of the polishing machines would be of help in acquiring a full understanding of their mode of operation. A few misprints appear in the text and formulae, but these will likely be obvious to the reader and cause no confusion. While the methods described in this book are often more adapted to commercial quantity production than to the making of single items, there is still much to be gained by even the casual laboratory worker.

This publication will be a valuable addition to the optician's bookshelf.

A. G. HALL
Massachusetts Institute of Technology

A Metric Based on the Composite Color Stimulus*

PARRY MOON, *Massachusetts Institute of Technology, Cambridge, Massachusetts*

AND

DOMINA EBERLE SPENCER, *The American University, Washington, D. C.*

1. INTRODUCTION

CONSIDERABLE attention has been devoted recently to the establishment of a metric by which the affine C.I.E. colorspace becomes a metric space.[1] In investigations of this kind, it has been customary to ignore the state of adaptation of the eye. But in some applications, visual adaptation is an important factor which must be taken into account.

A previous paper[2] presented a metric based on the MacAdam data.[3] The resulting metric space is of importance in all questions dealing with color discrimination and color tolerances. It does not apply, however, to problems dealing with large color steps such as are encountered in color harmony. Thus there is need for a color space which deals with large-step phenomena. The MacAdam data cover a large part of the chromaticity diagram; yet they give only a very limited range for the composite color stimulus[4] because the fovea was adapted in every case to nearly the coordinates of the test spot. Data for a much wider range of composite stimulus are given by the recent work of the Optical Society of America Subcommittee on the Spacing of the Munsell Colors.[5] The present paper describes a metric space which is based on the Munsell data and which takes adaptations into account.

The ω space results in a particularly simple representation of the Munsell system. The curves of constant hue appear as straight lines and the curves of constant chroma are uniformly spaced circles. This representation should be of value in any further revision of the Munsell system and in the extrapolation of the Munsell notation to the theoretical limits.[6]

2. METHODS OF REPRESENTING THE MUNSELL DATA

The Munsell system of color specification has been discussed exhaustively in this journal and will not be described here. The attempt in the original system was to obtain equal apparent steps between the chosen colors. Recently the O.S.A. Subcommittee on the Spacing of the Munsell Colors has attacked the problem of respacing these colors on the basis of the C.I.E. specification and on new data obtained with a large number of observers. One of the difficulties which they encountered is the peculiar shapes of the curves of constant hue and chroma in the C.I.E. chromaticity diagram. Figure 1 gives an example of the smoothed results for Munsell Value 5 and for the

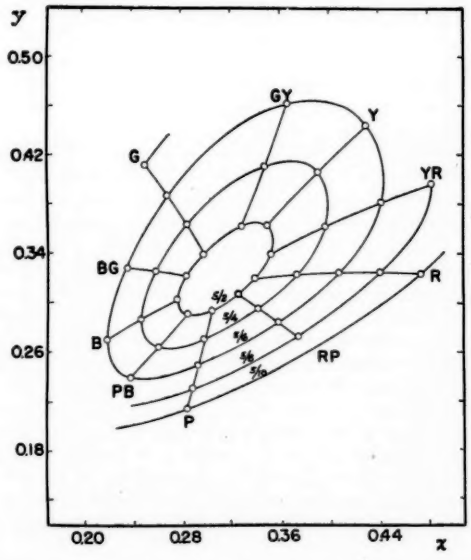

FIG. 1. Munsell data at Value 5, plotted in the C.I.E. chromaticity diagram.

* Based on a paper presented at the Winter Meeting of the Optical Society of America, New York City, March 5, 1943.

[1] L. Silberstein, J. Opt. Soc. Am. **28**, 63 (1938); **32**, 552 (1942); **33**, 1 (1943). D. L. MacAdam, J. Opt. Soc. Am. **33**, 18 (1943).

[2] D. E. Spencer, J. Opt. Soc. Am. **32**, 744 (1942). P. Moon and D. E. Spencer, J. Opt. Soc. Am. **33**, 260 (1943).

[3] D. L. MacAdam, J. Opt. Soc. Am. **32**, 247 (1942).

[4] D. E. Spencer, J. Opt. Soc. Am. **33**, 10 (1943).

[5] "Final report of the O.S.A. subcommittee on the spacing of the Munsell colors," J. Opt. Soc. Am. to be published.

[6] D. L. MacAdam, J. Opt. Soc. Am. **25**, 361 (1935).

principal hues (5R, 5YR, 5Y, 5GY, 5G, 5BG, 5B, 5PB, 5P, 5RP).

E. Q. Adams[7] developed a modified diagram in which the curves of constant chroma appeared more nearly circular than in the C.I.E. chromaticity diagram. The Adams diagram was used extensively by the Subcommittee in smoothing the original chroma data and in extrapolating to higher chromas. The data of Fig. 1 are replotted

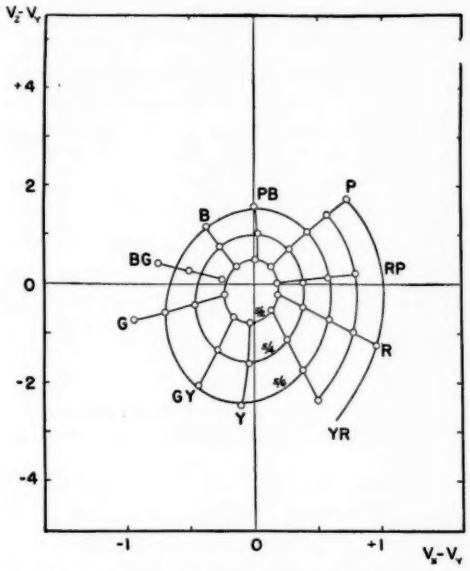

FIG. 2. Munsell data at Value 5, plotted in the Adams diagram.

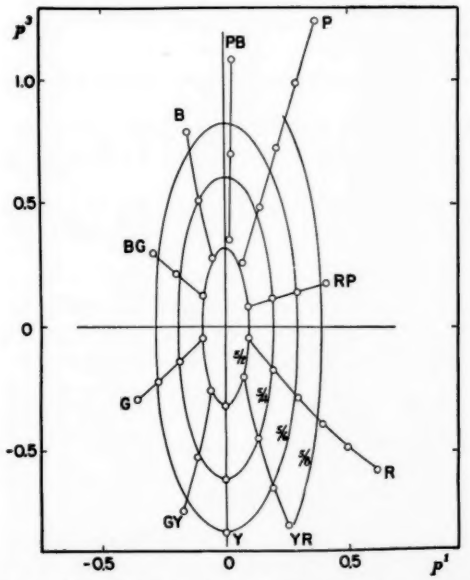

FIG. 3. Munsell data at Value 5, plotted in the p diagram for adaptation to a neutral gray surround.

[7] E. Q. Adams, J. Opt. Soc. Am. **32**, 168 (1942).

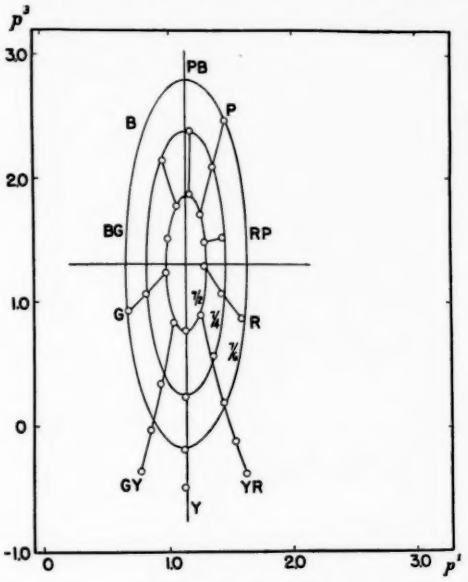

FIG. 4. Data at Value 7.

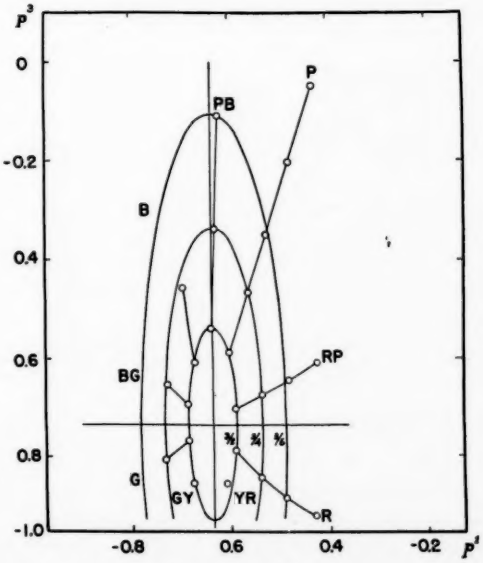

FIG. 5. Data at Value 3.

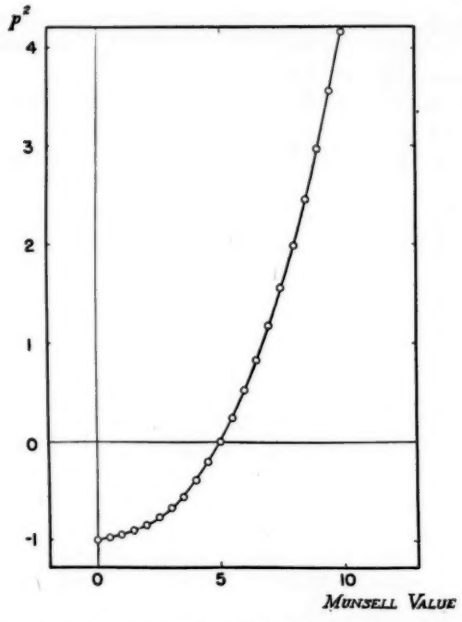

FIG. 6. Relation between p^2 and Munsell value. Points are Munsell data; curve is calculated from Eq. (6).

in the Adams diagram of Fig. 2. The curves of constant chroma are seen to be still far from circles and the Munsell hues are not represented by straight lines and are not evenly spaced.

To obtain the metric that is described in this paper, we first replotted the latest Munsell data[5] in terms of the composite color stimulus.[4] Use of this concept requires a knowledge of the state of adaptation under which the data were obtained. Records were available for three surrounds;[5] black, white, and gray; but in the final tables of the O.S.A. Report, results are given for a neutral surround of Value 5. Observations were made[5] with a series of small samples on a large neutral background and with rapid eye movements. Thus it seems reasonable to assume that the fovea was adapted to the neutral surround. The trichromatic coordinates of the surround were

$$x^1=19.19, \qquad x^2=19.77, \qquad x^3=20.10. \quad (1)$$

These numbers are based on $Y=100$ for MgO. Since the luminous flux density to the samples was approximately 600 lumens/m^2, the absolute values of X, Y, and Z could be given. However, the composite stimulus is unaffected by absolute magnitude, so it is permissible to use all data in the form given by the O.S.A. Subcommittee.

In accordance with the equations for the p tensor,[4]

$$p^1=\frac{xY/y-19.19}{19.77},$$

$$p^2=\frac{Y-19.77}{19.77}, \quad (2)$$

$$p^3=\frac{(1-x-y)Y/y-22.10}{19.77}.$$

The results of plotting the new Munsell data, in terms of the composite color stimulus, for three representative values are shown in Figs. 3, 4, and 5.

3. TRANSFORMATION TO EUCLIDEAN METRIC SPACE

The ellipses of Figs. 3, 4, and 5 can be transformed into circles. The minor semi-axes of the constant chroma ellipses are linear functions of p^1, the constant in the equation depending on the Munsell value. These constants were plotted as a function of p^2, and the resulting curve was fitted by the equation:

$$\text{Minor semi-axis} = 0.1680(1.630+p^2)^{\frac{1}{2}}-0.1190. \quad (3)$$

It is also found that the coordinates of the center of the sets of concentric ellipses are linear functions of p^2.

If the transformation is now made to a new ω space in which the unit of ω corresponds to one chroma step, then

$$\omega^1=\frac{2(p^1-0.950p^2)}{0.1680(1.630+p^2)^{\frac{1}{2}}-0.1190}. \quad (4)$$

In a similar manner, it is found that

$$\omega^3=\frac{2.270(p^3-1.100p^2)^{1.20}}{0.6280(1.800+p^2)^{\frac{1}{2}}-0.5210}. \quad (5)$$

The points of Fig. 6 show the latest data on Munsell value, while the curve is a plot of the equation,

$$\text{Value}=5.0(p^2+1)^{0.426}. \quad (6)$$

According to Bellamy and Newhall,[8] 50 minimum perceptible value steps correspond to 6 minimum perceptible chroma steps. It is convenient to introduce this ratio into our ω space, giving

$$\omega^2 = 41.70(p^2+1)^{0.426}. \qquad (6a)$$

The new ω space is a Euclidean metric space in which unit distance corresponds to one Munsell chroma step. By means of it, a metric is introduced into the affine p space for the range of values covered by the O.S.A. Subcommittee data. This metric was obtained by the same general procedure used in establishing a metric on the basis of the MacAdam data.[2] The two describe different conditions and are in no way inconsistent.

Figure 7 shows the same O.S.A. data for Value 5 transformed to ω space by means of the foregoing equations. Equally spaced concentric circles are drawn to represent the curves of constant chroma.[9] The points are seen to be in good agreement with these circles except in the purple and purple blue, where the use of the Adams diagram by the Subcommittee may have resulted in some distortion.

It will be noted also (Fig. 7) that points representing the same hue fall approximately on a straight line through the origin of coordinates. The solid lines are drawn to fit the Munsell data, while the dotted lines are equally spaced at angles of 36°. The yellow, green yellow, and blue points are in excellent agreement with this uniform spacing, while the other hues are not greatly in error. Even these discrepancies may well be justified, since the methods of the O.S.A. Subcommittee were not designed primarily to respace the hues but only to smooth the data. Figures 8 to 12 show similar diagrams for the other Munsell values. It should be noted that in developing the metric, we have used the smoothed data[5] (which are based on experiment) but not the extrapolated results given in the Subcommittee report.

It is not certain that a relocation of the Munsell hues is justified on the basis of the new metric. But the designation of equal hue steps seems to be inherently on a less secure foundation than the designation of value or chroma steps. In particular, the diagram seems to indicate that the Munsell G and BG are too close together, as are the R and RP. An experimental investigation of this point might lead to interesting conclusions.

The advantage of the ω diagram over previous methods of plotting Munsell data is that it gives a simple, uniformly spaced, orthogonal mesh in which discrepancies are easily noted. The diagrams for different values are all of the same size, so that Figs. 7 to 12 can be superposed and any differences in the locations of the points can be instantly detected. A few such discrepancies (which are not recognizable in previous diagrams) are as follows:

slight tendency for B/2 to lie too close to the center of coordinates at all values;
B/6 is consistently too purple at all values;
R/2 seems to be slightly purple in comparison with other reds;
PB and P at the higher chromas appear to be too unsaturated (as noted previously);
Value 2 results are erratic, probably because of experimental difficulties.

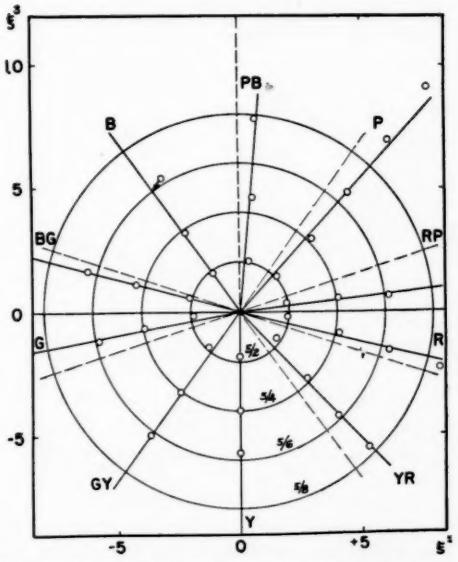

FIG. 7. Munsell data at Value 5, plotted in the ω diagram.* Heavy radial lines are drawn to fit the latest Munsell data. Dotted radial lines are for equal hue spacing on the basis of the ω diagram (36° angular spacing).

[8] B. R. Bellamy and S. M. Newhall, J. Opt. Soc. Am. **32**, 465 (1942).

[9] These circles do not necessarily correspond exactly to the ellipses of Fig. 3 because of the smoothing process resulting from the use of Eqs. (4) and (5).

* To agree with the notation used in the text, the ξ's in this and subsequent figures should be ω's.

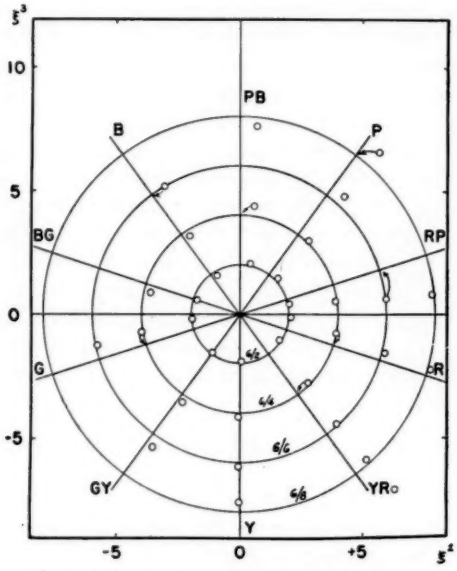

FIG. 8. Munsell data at Value 6. Radial lines are equally spaced.

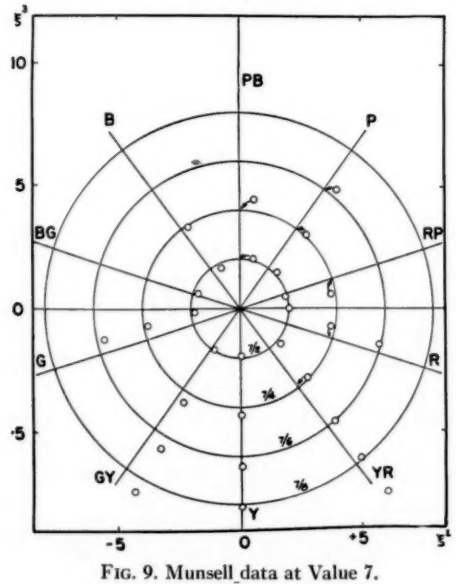

FIG. 9. Munsell data at Value 7.

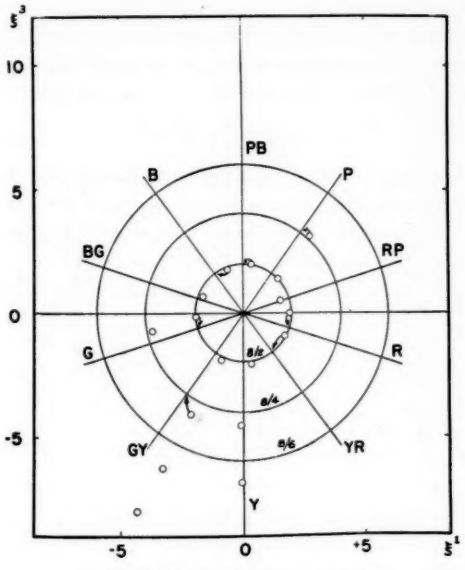

FIG. 10. Munsell data at Value 8.

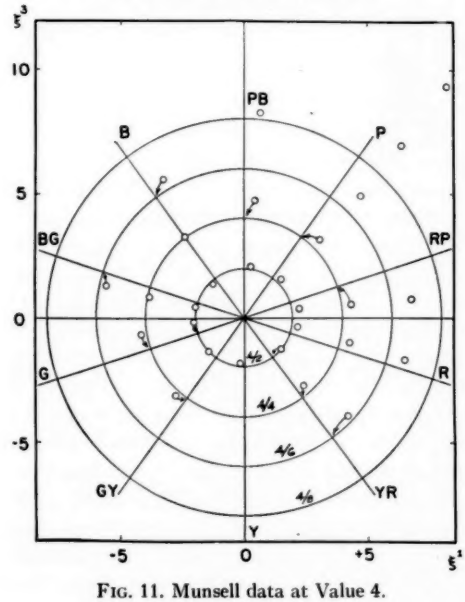

FIG. 11. Munsell data at Value 4.

The foregoing discussion should not be construed as a criticism of the Munsell system or of the splendid work of the O.S.A. Subcommittee. The Munsell system provides what is undoubtedly the greatest collection of large-step color-discrimination data, and for that reason it was employed in our investigation of a metric space suitable for scientific investigations of color harmony. Incidental to this study was the conclusion that the new metric would be of practical value in the further development of the Munsell system itself.

4. A METHOD OF EXTRAPOLATING THE MUNSELL DATA

The Munsell papers are limited in chroma and value by available colorants, but it is desirable to be able to extrapolate the Munsell notation to apply to any theoretically realizable pigment. In Section 3, it was shown that the curves of constant chroma may be represented by circles in the $\omega^1\omega^3$ planes and that the curves of constant hue may be represented by radial lines in these planes. The geometric simplicity of this arrangement allows a straightforward extrapolation of the Munsell notation to any chroma.

Given hue, chroma, and value; to determine the C.I.E. coordinates x and y. Evidently,

$$\omega^1 = C\cos\theta, \quad \omega^3 = C\sin\theta, \quad \omega^2 = 8.33V, \quad (7)$$

where C = Munsell chroma,
V = Munsell value.

For equal angular spacing of hues in the ω diagram, the angle θ has the following magnitudes for the ten principal hues:

5RP, 18°; 5P, 54°; 5PB, 90°; 5B, 126°;
5BG, 162°; 5G, 198°; 5GY, 234°; 5Y, 270°;
5YR, 306°; 5R, 342°.

Intermediate hues are obtained in a similar manner. In case an unequal hue spacing is desired, the angles can be read from Fig. 7.

Then from Eqs. (4), (5), and (6a),

$$p^2 = \left(\frac{\omega^2}{41.70}\right)^{2.35} - 1, \quad (8)$$

$$p^1 = 0.950p^2 + \frac{\omega^1}{2}[0.1680(1.630+p^2)^{\frac{1}{2}} - 0.1190], \quad (9)$$

$$p^3 = 1.100p^2 + \left\{\frac{\omega^3}{2.270}[0.6280(1.800+p^2)^{\frac{1}{2}} - 0.5210]\right\}^{0.833}. \quad (10)$$

Equations (8), (9), and (10) give the p tensor corresponding to any given hue, value, and chroma, irrespective of whether this point in ω space corresponds to a realizable Munsell color.

But a given p^i can be obtained in infinitely many ways, depending on visual adaptation. If adaptation is fixed by the specification of x^1, x^2, x^3, the C.I.E. coordinates of the foveal adaptation,[4] then the equations

$$p^1 = (X - x^1)/x^2,$$
$$p^2 = (Y - x^2)/x^2, \quad (11)$$
$$p^3 = (Z - x^3)/x^2,$$

may be used. Thus the C.I.E. coordinates of the test spot are

$$X = p^1x^2 + x^1, \quad Y = p^2x^2 + x^2, \quad Z = p^3x^2 + x^3. \quad (12)$$

The position of the point in the chromaticity diagram is therefore designated by

$$x = \frac{p^1x^2 + x^1}{(x^1+x^2+x^3) + x^2(p^1+p^2+p^3)},$$
$$y = \frac{x^2(p^2+1)}{(x^1+x^2+x^3) + x^2(p^1+p^2+p^3)}. \quad (13)$$

The foregoing equations provide a given Munsell color with different C.I.E. specifications, depending on the adaptation of the eye. In most cases, however, the practical convenience of having a one-to-one correspondence between p space and C.I.E. space overbalances the resulting loss in generality. If viewed on a large neutral gray

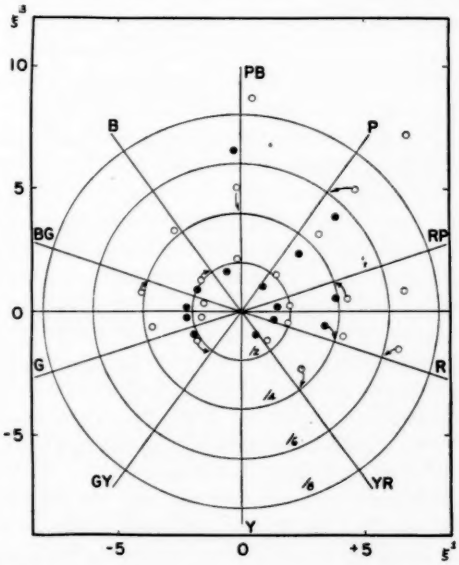

FIG. 12. Munsell data at Values 2 and 3. White circles, Value 3; black circles, Value 2.

surround specified by Eq. (1), the Munsell colors are seen with respect to this state of adaptation, and Eq. (13) becomes

$$x=\frac{19.77p^1+19.19}{61.06+19.77(p^1+p^2+p^3)},$$
$$y=\frac{19.77(p^2+1)}{61.06+19.77(p^1+p^2+p^3)}. \tag{14}$$

5. RELATION BETWEEN TWO METRICS

The question arises as to the relation between the present metric and the one[2] based on the MacAdam results. To answer this question, one must consider the methods employed in obtaining the two sets of data. Information on minimum-perceptible steps is obtained by use of a two-part field covering at least the entire fovea. Under ideal conditions the surround is made identical in helios and chromaticity with one of the half-fields; and when a color match is obtained, the whole field of view appears essentially uniform. Thus there is no question as to the state of adaptation of the fovea. Even when the surround is different from the test field, as in the MacAdam work, the observer continues to concentrate on the boundary line between the two half-fields and his foveal adaptation remains nearly the same as before.

To obtain an adaptation state that is distinctly different from that produced by the test spot, one may expose the latter for only an instant and keep the observer adapted to a large, uniform surround. Or one may leave test spots in the field of view but make them so small that they have negligible effect on adaptation. In either case, the fine discrimination obtainable with the previous arrangement is no longer possible and the MacAdam data are inapplicable. Thus the MacAdam data are not well adapted to representation in p space.

On the other hand, the metric described in the present paper deals with large color steps and is associated inherently with adaptation space. One method of obtaining information with large color steps is to present the observer with two different color patches on a large uniform background. The observer decides what intermediate patch bisects the color interval between the two given samples. A modification of this procedure deals with the experimental establishment of a scale of equal steps of chroma or value, as in the Munsell system. In either case, the observer finds it necessary to move his eyes rapidly over the whole ensemble, and the fovea tends to adapt itself to an intermediate condition. If the samples are small and are well separated on a medium gray background, the fovea will tend to adapt itself to the background, as was assumed in dealing with the Munsell data. If other backgrounds are used, it is found that the uniform scales previously obtained must be altered, as shown in the experiments of the O.S.A. Subcommittee. The results of such large-step experiments depend on the state of foveal adaptation and should, therefore, be specified in p space rather than in C.I.E. space. A metric is introduced into this p space, giving the simple Euclidean ω space described in the present paper.

The new metric in no way supersedes the one based on the MacAdam data. Both are useful but in entirely different fields. The ξ space can be employed in all questions dealing with the discrimination of small color differences between rather large contiguous samples. It applies to questions of color tolerance in the manufacture of textiles, tiles, and other materials and it specifies the precision of heterochromatic visual photometry. The j.n.d. at any point in the 3 space and in any direction is specified by the same geometric distance, which correlates a great number of data in a very simple geometric manner. Large color distances are measured directly off the ξ diagram, the unit of measurement being either the MacAdam standard deviation or the j.n.d., *with readaptation at each step*. Large color differences expressed in this way have no apparent connection with color differences judged at a fixed adaptation, such as are used in the Munsell system and in color harmony.

The ω space also represents equal color steps in any direction by equal distances in the 3 space. However, the whole diagram is based on a fixed state of adaptation, and the positions of all the familiar landmarks (spectral locus, for instance) change if the adaptation changes. Small distances in the ω space correspond to what might be measured with a fixed state of foveal adaptation, and these distances have no known relation to j.n.d.'s measured in the usual way with readaptation at

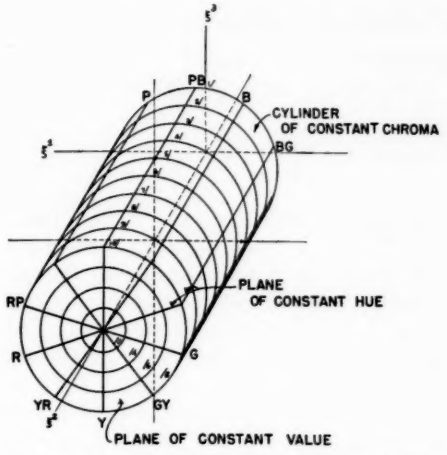

FIG. 13. The three-dimensional ω space. Adaptation is to a neutral gray of Value 5.

each step. The ω space should be important in the future development of scientific color harmony. It gives also a representation of the Munsell system—a representation which is believed to be simpler, more exact, and more suggestive of ways for improvement than any previous diagram. Furthermore, the new space provides a logical method of extending the Munsell notation beyond the range of present pigments. Thus each of the two metric spaces (ξ space and ω space) has its own characteristics and its own applications.

Despite the differences between the two sets of experimental data, there still remains a possibility of describing both of them in terms of a single metric in p space. Even though the adaptation changes at each point in ξ space, the composite stimulus can still be computed and the metric coefficients can be expressed in terms of the composite stimulus. When this is done, the MacAdam data are found to lie within the ellipse of Chroma 2 in p space. The Munsell data all lie on or outside this ellipse. Mathematically, it would be possible to define a single metric covering the two sets of data. Since the practical applications are not great, however, the significance of such an extension would be largely academic.

6. SUMMARY

Any scientific treatment of color harmony will require for its foundation an adequate metric colorspace. Moreover, this colorspace will have to deal with large-step phenomena rather than with minimum perceptible color differences, for small color steps tend to be ambiguous and therefore inharmonious aesthetically.

In obtaining a space for color harmony, we took the affine p space or adaptation space developed in a previous paper[4] and introduced a metric based on the latest Munsell data. The unit in this new ω space is equal to one Munsell chroma step, and equal distances in any direction represent psychologically equal color steps. The ω space is a Euclidean 3 space (Fig. 13). For a given adaptation, surfaces of constant helios are parallel planes, surfaces of constant hue are planes that contain the ω^2 axis, while surfaces of constant chroma are concentric circular cylinders.

The state of foveal adaptation is representable by three numbers giving the C.I.E. coordinates of an equivalent uniform field.[4] This adaptation point conditions the whole relation between the psychological color specification and the C.I.E. specification. If, however, one fixes on a definite state of adaptation (as obtained by use of a specific large gray surround and rapid eye movements) there is obtained a one-to-one correspondence between points in C.I.E. space and in ω space.

The simplicity of the resulting representation of the Munsell system in ω space is of importance in the further rationalization of that system and in the extrapolation of Munsell notation to hitherto unexplored chromas.

In conclusion we gratefully acknowledge the help of the O.S.A. Subcommittee on the Spacing of the Munsell Colors. We are thankful particularly to Dorothy Nickerson for her continued interest and for her material aid in the interpretation of the Munsell data. Suggestions were also received from Deane B. Judd and P. G. Nutting, to both of whom we extend our thanks.

JOURNAL OF THE OPTICAL SOCIETY OF AMERICA VOLUME 33 NUMBER 5 MAY, 1943

An Empirical Approach to Lens Designs

The Huygens Eyepiece

W. M. STEMPEL
Stevens Institute of Technology, Hoboken, New Jersey
(Received April 15, 1943)

INTRODUCTION

THE problem of designing properly functioning optical systems has stimulated a number of different approaches of which three have now received general recognition.

One of these approaches is due to Conrady, the foundation of which is most skillfully and interestingly presented in his own book, *Applied Optics and Optical Design*. His method consists of an efficient combination of first-order equations with preliminary ray tracings to produce the best possible first approximation. Relatively simple differential corrections can then be applied to bring the design fully in accord with specifications.

The other two methods of solving optical design problems give rise to working equations designated as "third-order" equations since third-order effects are retained. The results are certainly no better than, if even as good as, the results obtained by Conrady's method so that the final set of ray tracings and differential corrections are still necessary.

The working equations of both these last two "third-order" methods can be derived from the general equations of Schwarzchild, and in fact have been proven to be identical except for the choice of parameters used.

One of these third-order methods is used by Koenig and appears in the German literature. Some writers call this system the, "Continental system." The other system is due to H. Dennis Taylor and is based on the work of Coddington, whose work Taylor greatly extended. The latter will be referred to in this article as the Taylor system, and the German system which is less simple in form and has no advantage over the Taylor system will not again be referred to.

All that can be expected from any of these different analytical approaches is a fairly close approximation to the desired optical system. This unfortunate state of affairs is due to the intimate combination of two causes; the fact that the rigorous analysis of these optical problems leads to equations much too complex to be of any practical value and so have to be simplified by various approximations, and the fact that these approximations introduce uncertainties in the final intersecting lengths and angles, from which the aberrations are obtained, which are often many times larger than the aberrations themselves. It therefore becomes necessary to make a final check of all aberrations, and to reduce them to permissible magnitudes, by trigonometric ray tracing.

The above described preliminary calculations are very laborious and time consuming. The writer, realizing that only approximations to the desired systems are possible by the use of these equations, became deeply interested in the possibility of shortening these preliminary operations by some empirical method. Attempts made with telescopic systems using a Huygens eyepiece were so successful that it seemed very desirable to publish the work done to date immediately. The method will be extended, if possible, to other systems in future articles.

GENERAL THEORY

For thin lenses the focal length of the eyepiece (f_e') is given in terms of the focal length of the eye lens (f_A'), the focal length of the field lens (f_B'), and the distance between the posterior principle point of the eye lens and the anterior principle point of the field lens (a) by

$$f_e' = (f_A' f_B')/(f_A' + f_B' - a). \quad (1)$$

Conrady also gives an equation for determining the distance between the lenses of a Huygens eyepiece in terms of f_A', f_B', and l'_{prB} (the distance of a thin objective of a telescope from the posterior surface of the field lens of the eyepiece), which will reduce the transverse chromatic aberration to zero as

$$a = (f_A' + f_B')/[(2 - f_B'/l'prB]. \quad (2)$$

Recalling that for a telescopic system $f_e'+f_0'=l'_{prB}$ plus the distance between the posterior Gaussian plane of the eyepiece and the posterior surface of the field lens of the eyepiece, and substituting into this equation the values of the last two terms [the second is $=af_B'/(f_A'+f_B'-a)$], we get after reduction

$$f_e'+f_0'=\frac{a^2f_B'}{[f_A'+f_B'-a][2a-(f_A'+f_B')]}, \quad (3)$$

where f_0' is the focal length of the telescope objective with which the eyepiece is to be used.

Equation (3) brings out the following facts:

When $f_A'+f_B'=a$, $f_e'+f_0'=\infty$. From Eq. (1) we see that this means that $f_e'=\infty$ and thus determines the maximum value of a. When $f_A'+f_B'=2a$, $f_e'+f_0'$ is again infinite. This can only occur for $l'_{prB}=\infty$, and means that $f_0'=\infty$, and gives the other limiting value of a, the minimum value. The possible values of a are thus quite limited and, if one considers further the impracticability of values of a resulting in large values of f_e' and f_0', the range is further reduced to only a small part of that indicated by the above analysis.

The minimum l'_{prB} is obtained when

$$a=\tfrac{2}{3}(f_A'+f_B')$$

which in turn gives

$$l'_{prB}=2f_B'. \quad (4)$$

Telescopic systems are never as short as this, and since the useful range will lie between this and ∞, corresponding to values of a between $\frac{2}{3}(f_A'+f_B')$ and $\frac{1}{2}(f_A'+f_B')$, the extreme variation in a is less than 30 percent. The other side of the minimum corresponds to long focus eyepieces, and, therefore, low magnification and is of little practical value. When the thickness of the lenses is taken into account the range of a is moved toward the $\frac{1}{2}(f_A'+f_B')$ value, sometimes actually overlapping this point. The above facts account for the unusual success attained in the past by the use of the so called "textbook" formula for the elimination of chromatic aberration, namely,

$$a=\tfrac{1}{2}(f_A'+f_B').$$

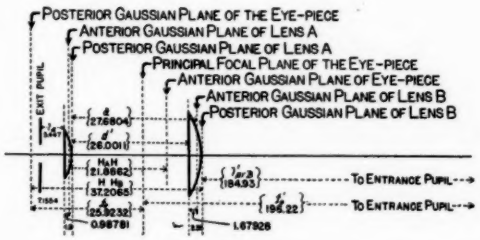

FIG. 1.

Note: This diagram was prepared from left to right tracing data except that the entrance pupil and exit pupil were interchanged for convenience in the final discussion on the aberrations of these eyepieces. The numbers apply to the particular eyepiece given special consideration. .

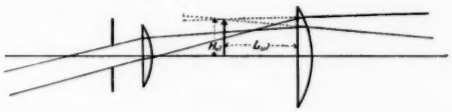

FIG. 2.

This smallness of the useful range of a makes the empirical approach, to be described in the following paragraphs, particularly effective, as will be clearly apparent.

THE PREMISES

We shall choose for this experiment a borosilicate crown glass and an ordinary crown glass whose indices of refraction, according to Bausch and Lomb, are, respectively,

$$N_d=1.51700 \quad N_f=1.52262 \quad N_c=1.51461$$
$$1.54110, \quad 1.54746, \quad 1.53842.$$

We shall also choose Conrady's "three ray method" of designing eyepieces. (This method is briefly described as follows: Instead of tracing a paraxial and a marginal ray for determining the spherical aberration and two more, associated with appropriately chosen indices, at 0.7071 of maximum aperture, Conrady compromises both aperture and indices. He takes rays associated with appropriate indices at 0.8 aperture and uses one of these with a paraxial ray of the same index for determining the spherical aberration. This saves the tracing of one ray and when properly used gives results quite equal to the four ray method.) The appropriate indices for the borosilicate crown indicated by this method are determined as follows:

$$N_d= \qquad 1.51700$$
$$+0.188(N_f-N_c) \qquad 0.00151$$
$$N_y \quad \text{(the longer wave-length} \quad =1.51851 \quad (5)$$
$$+(N_f-N_c) \qquad 0.00801$$
$$N_v \quad \text{(the shorter wave-length)}=1.52652. \quad (6)$$

TABLE I.

Focal length ratio	Thickness of Eye lens	Thickness of Field lens	O.S.C.′	Inside air space d'	Separation adjustment coefficient	Air space adjustment coefficient	Over-all angular magnification	Axial chromatic constant	Focal length of the associated objective	Focal length of the eyepiece
				Borosilicate crown glass						
1.4	1.5	2.1	0.00114579	24.87553 (24.87530)	1.13136	1133	−3.893	0.0009998	101.21	26.0001
1.7	1.5	2.55	0.00117227	26.00108 (26.00069)	1.060104	1301	−7.569	0.0009997	196.22	25.9232
1.9	1.5	2.85	0.00119087	26.72600			−14.14	0.001003	365.68	25.861
2.0	1.5	3.00	0.00119431	27.08800 (27.08923)	1.001834	1536	−22.38	0.001001	578.2	25.8349
				Ordinary crown glass						
1.4	1.5	2.10	0.00121128	24.02486 (24.03086)	1.17137	909	−3.658	0.001007	92.33	25.2358
1.7	1.5	2.55	0.00124024	25.1587 (25.1606)	1.07472	1126	−6.710	0.001002	169.05	25.1625
2.0	1.5	3.00	0.00126430	26.25540	1.01729	1284	−16.21	0.0009989	406.5	25.0771

Note: The second value for d', the one in brackets, has been more completely corrected for transverse chromatic aberration by the use of the coefficient in column seven.

Tracing will be carried out from eye lens to field lens, see Fig. 1 or 2.

$R_1 = \infty$ for the Huygen's eyepiece. R_2 will be given the value of 10 mm. This value is convenient in the numerical calculation and gives an eyepiece of usable dimensions (about one inch focal length). The design can of course be easily changed to other sizes by proportion. $R_3 = \infty$ and $R_4 = (f_B'/f_A')R_2$.

With the above chosen values of N_d and R_2 the focal length of the eye lens of the eyepiece is

$$f_A' = R_2/(N-1) = 19.3424 \qquad (7)$$

and the focal length of the field lens is

$$f_B' = (R_4/R_2)f_A'. \qquad (8)$$

The eyepiece will be assumed to have a semi-field of (17.5°). The zonal correction will therefore be made for 14°. According to Conrady, the coma will be acceptable if the "Offense Against the Sine Condition" (O.S.C.) (absolute sagittal coma in the image plane divided by the distance of the image point from the axis of the system) is not allowed to exceed 0.0025. The transverse chromatic aberration will be satisfactory if the coefficient for the transverse chromatic aberration (g_7 in Conrady's equation for the transverse chromatic aberration = $g_7 \times$ distance of the image point from the axis) in the paraxial region is made equal to 0.00100.

DETERMINATION OF THE EMPIRICAL DATA

The basis for the empirical procedure about to be described is the collection of end results taken from the tracings of a set of standard rays traced through the Huygen's eyepiece for each of several values of f_B'/f_A' and for the corresponding best distance of separation, the f_B'/f_A' ratio being varied through the useful range. From these the numerical values for the following quantities, which will appear in the Conrady equations following, were obtained.

U_y' = the angle which the emerging marginal ray of the light of longer wave-length makes with the axis of the system.

u_y' = the angle which the emerging paraxial ray of the light of longer wave-length makes with the axis of the system.

u_v' = the angle which the emerging paraxial ray of the light of shorter wave-length makes with the axis of the system.

L_y' = the distance of the axial intersection of the marginal ray of the light of longer wave-length from the last lens.

l_y' = the distance of the axial intersection of the paraxial ray of the light of longer wave-length from the last lens.

l_v' = the distance of the axial intersection of the paraxial ray of the light of shorter wave-length from the last lens.

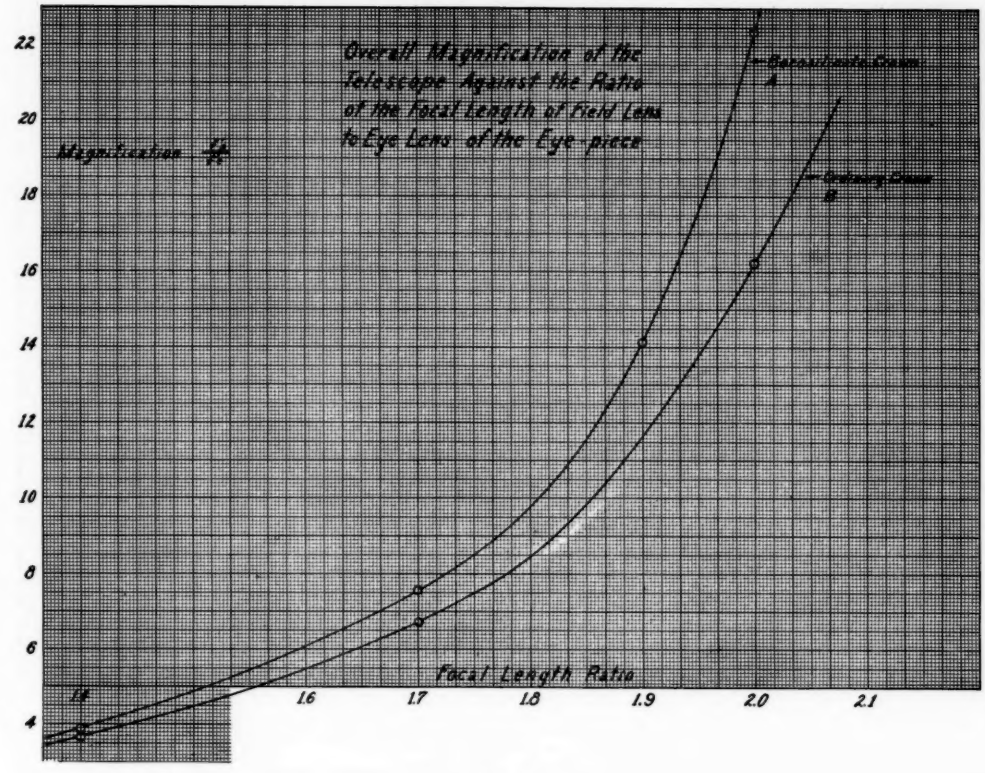

FIG. 3.

Conrady found that for eyepieces using a total field of not more than 40° the coma will, in general, be held to tolerable amounts and will be distributed uniformly from center to edge of the field if

$$\text{O.S.C. is about } 0.2 \sin^2 U'. \tag{9}$$

The focal length of the telescope objective to be used with each eyepiece meeting the above coma condition will be given by

$$f_0' = \frac{(l_y' - L_y')(1 - \text{O.S.C.}')}{u_y'/\sin U_y' - (1 - \text{O.S.C.}')}, \tag{10}$$

the over-all magnification of the telescope by

$$MA' = -f_0'/f_e', \tag{11}$$

and the transverse chromatic constant by

$$g_7 = \frac{u_v' - u_y'}{u_v'} + \frac{u_y'}{u_v'} \frac{l_y' - l_v'}{f_0' + l_y' - l_v'}. \tag{12}$$

Tracing a marginal (aperture 4 mm) and a paraxial ray for the N_y ray, parallel to the axis of the system, for each of the eyepiece focal length ratios (f_B'/f_A') and a third ray (also parallel to the axis) for the more refractive ray (N_v), Table I is obtained for the various quantities in the last medium.

First column. This column gives the ratio of the focal length of the field lens of the eyepiece to the focal length of the eye lens.

Second and third columns. These two columns give the thicknesses of the eye lens and the field lens, respectively. These values are those commonly found in eyepieces but the effect of changes will be studied later on in this article.

Fourth column. This column gives the "Offense against the sine condition" (O.S.C.') worked out to the full precision corresponding to six places in the value of the index of refraction.

Fifth column. This column gives the proper

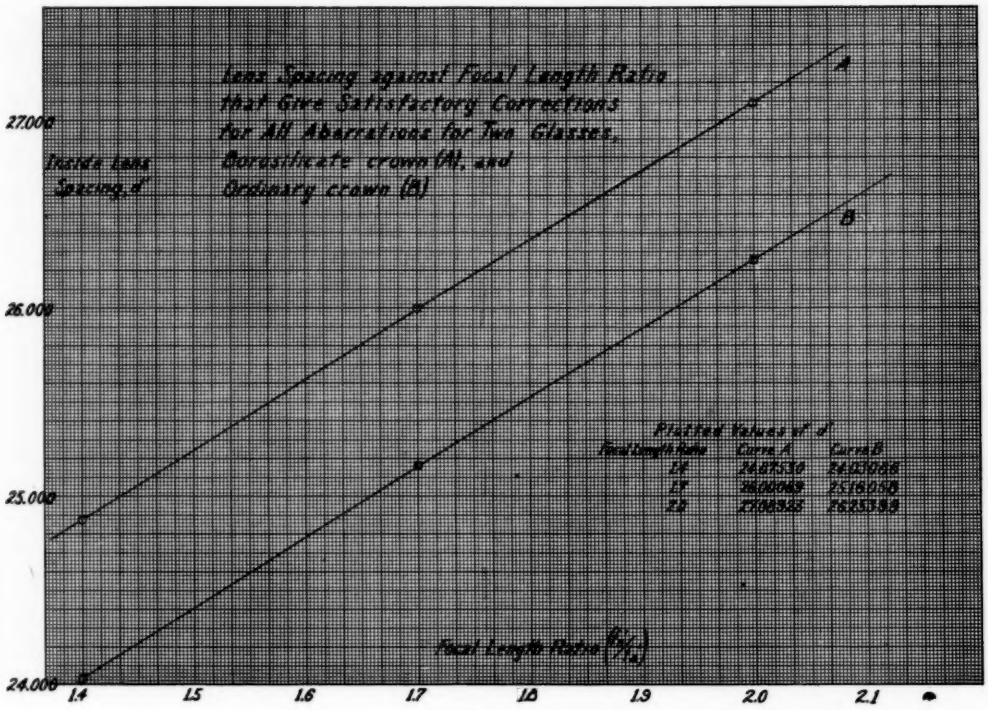

FIG. 4.

space between the inside surfaces of the eye lens and the field lens of the eyepiece for full transverse chromatic correction at 14°. For research purposes these are given to a higher degree of precision than required in practice. If these distances are taken in mm the eyepiece is, as a whole, almost of the proper size and since precisions better than 0.03 mm are rarely achieved in the glass shops, the last three digits could be dropped for practical purposes. It may be of interest to say that a change of 0.1 mm in d' produces about a 10 percent change in g_7 and a 3 to 5 percent change in magnification, inverse in both cases. This point will be examined in more detail later.

Sixth column. This column contains a coefficient which the writer has designated as the "Gaussian plane separation adjustment coefficient." This is a coefficient which when multiplied into $(f_A'+f_B')/2$ gives the proper distance between the posterior Gaussian plane of the eye lens and the anterior Gaussian plane of the field lens. When the distance of the anterior Gaussian plane of the field lens from the anterior lens surface (l_{ppB} = thickness of the lens divided by the index of refraction for plano convex lenses) is subtracted from the above, the result is the air space between the eye lens and the field lens. This calculation is not generally necessary since the latter distance d' can be read directly from the curve. It may be occasionally useful to the researcher when higher precision than is forthcoming from the curves is desirable. It will also be found useful when a region more or less remote from that covered by this investigation is to be studied.

Seventh column. This column has been called the "Air space adjustment coefficient." This quantity is the first derivative of d' with respect to g_7, $-dd'/dg_7$. Should one, by the simple procedure previously indicated, arrive at a prescription which, when tested by ray tracing, is found to have more or less transverse chromatic aberration than desirable, the prescription can be quickly corrected by multiplying the amount of correction to be made by this coefficient and

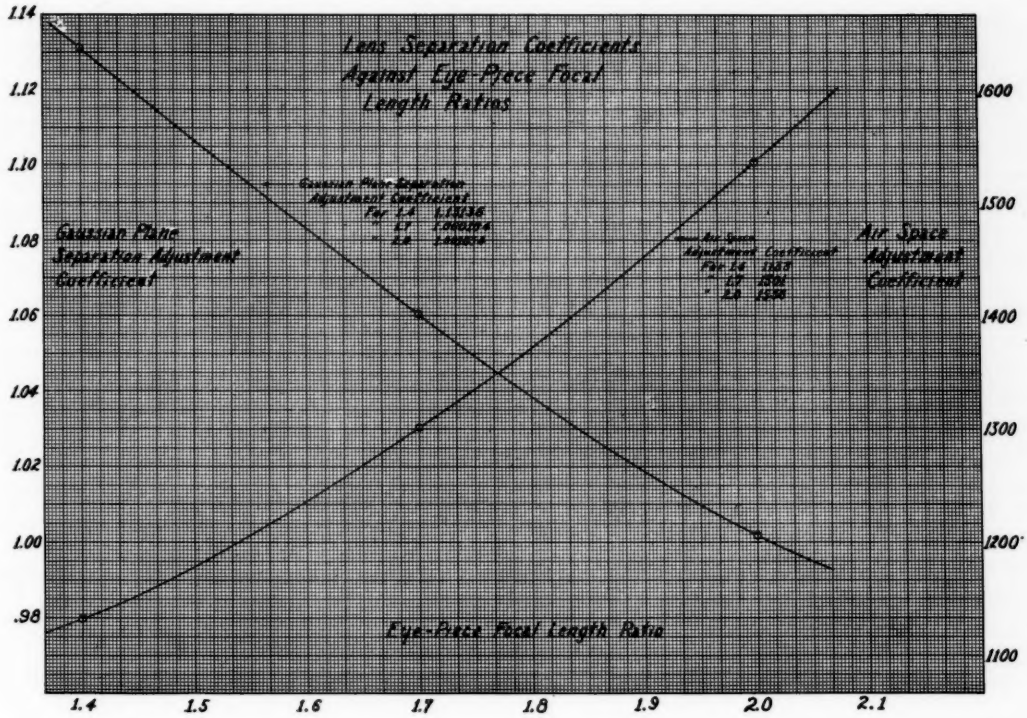

FIG. 5.

adding this quantity to, or subtracting this quantity from, the incorrect value of d' depending on whether the g_7 is too large or too small (the variation is here an inverse one).

Eighth, ninth, tenth, and eleventh columns. These are, respectively, the over-all magnification of the telescope, the transverse chromatic aberration proportional to the first power of the off-axis displacement of the image point, the focal length of the objective which will give the coma indicated in column four, and the focal length of the eyepiece, all given to a precision consistent with six places in the index of refraction.

The Curves

Curves may now be plotted from the data given in this table, the size of the curves depending on the precision required (see Figs. 3–5). These curves make it possible to determine the details for the prescription for any desired eyepiece without the need of any tracing or calculating as will be explained presently. If, however, the precision demands curves unpractically large, it is still possible to compute quickly the desired quantities from the data given in this table, as will be made clear later.

The following information is directly deduced from the curves.

Lens Spacing Against Focal Length Ratios

The air space between components of the eyepiece grows larger as the focal length ratio increases. The change seems quite linear and of appreciable value. Changing to glass of a different index of refraction results in an almost uniform change in the spacing throughout the range of focal length ratios in common practice, smaller for glass of a higher index and thus leading to more compact eyepieces. Knowing the change in d' resulting from a known change in the index of refraction the proper value of d' for any new glass choice is quickly and easily calculated for all changes of index likely to be met with.

Over-All Magnification of Telescopic Systems

The magnification grows rapidly larger as the focal length ratio increases. (The magnifications are plotted as if positive in this curve for easier interpretation. It must be kept in mind that, as shown in the table, these magnifications are always negative for telescopic systems of the type here studied.) This increasing magnification with increasing focal length ratios (f_B'/f_A') is most striking, especially in the neighborhood of the ratio 2 and for the borosilicate glass. This accounts for the wide range of usefulness of eyepieces with this value of focal length ratio. However, as focal length ratios increase, the range of possible transverse chromatic correction decreases and so, while at 2 there is still plenty of range for adjustment, at a focal length ratio of 2.3 the possible chromatic correction for the same coma correction has dwindled to zero. This condition does not occur so soon in the case of the ordinary crown glass and so we find, in earlier eyepieces, focal length ratios as high as 3.

Lens Separation Coefficients

The law of change of these coefficients is clearly apparent from the curves so that these coefficients can be quickly determined for any focal length ratio for the entire range ever likely to be considered. It is interesting to note that the value of this coefficient is practically 1 in the neighborhood of the focal length ratio 2 and again demonstrated why the so-called textbook formula for the correction of chromatic aberration, $\frac{1}{2}(f_A'+f_B')$, has always been so satisfactory in this region.

The air space adjustment coefficient slopes the opposite direction from the Gaussian coefficient and takes on a value which looks rather large, especially in the neighborhood of a focal length ratio of 2. Since, however, it is to be applied to a prescription already fairly good, it will be multiplied by a relatively small number and so gives no trouble.

Utilization of the Curves

The method to be followed in making use of the above given empirical data will now be described.

The magnifying power of a telescope is usually the starting point of telescope designs. For this case the steps would be as follows:

1. From the "Magnification-focal length ratio" curve, determine the proper focal length ratio to be used.

2. From the "Focal length ratio—d'" curve, determine the proper d' corresponding to the focal length ratio determined in (1).

3. Assuming the choice of glass and the size, indicated by f_e' and R_2 (=10 mm), as satisfactory, all data are now available to write down, without having to trace any rays or having to do any computing, the complete prescription, and with full confidence that the coma (O.S.C.′ about 0.0012) is well within acceptable tolerances (O.S.C.′=0.0025), and that the paraxial transverse chromatic aberration constant g_7 is about 0.00100 and, therefore, the chromatic aberration itself practically zero at 14° from the axis, and all other aberrations about one-half the maximum tolerances.

Example

Assuming a magnification of 7.56 we find that the focal length ratio should be 1.7. This in turn calls for $d'=26.005$. Now assuming 1.5 mm for the thickness of the eye lens and $1.5\times1.7=2.55$ for the thickness of the field lens, values used in preparing these data, the full prescription would be written down as:

$$\infty$$

1.5 mm

10 mm

26.005 mm

$$\infty$$

2.55 mm

17 mm

Should it be desirable to change the size of the eyepiece from the one just indicated, it will only be necessary to change proportionately all linear quantities, including, of course, the focal length of the objective with which the eyepiece is to be used. The magnification will remain unchanged. Changes to be made in other factors will be discussed later in connection with the full analysis of a particular case and after presenting a set of slide-rule calculating formulas intended for making rapid differential corrections to almost completed designs.

Slide Rule Correction Equations

Whenever there still remain small amounts of aberration in a given optical design, the differential calculus is extremely helpful, provided, of course, that the limitations of this method of approach are always kept in mind, namely, that the changes must be small relative to the intersecting lengths and angles themselves.

We start with the two general ray tracing equations

$$L'-r=\frac{N}{N'}(L-r)\frac{\sin U}{\sin U'}$$

and

$$U'=U+I-I',$$

where r is the radius of curvature of the refracting surface, U the angle the incident ray makes with the axis of the system, and L the distance from the surface to the axial object point, the primed letters referring to the ray after refraction and the unprimed letters to the ray before refraction.

The calculus applied to these equations gives, after considerable reduction, the following equations.

	For curved refracting surfaces:	For plane refracting surfaces:
$\frac{\partial U'}{\partial U}$	$=1+\cot U\frac{\sin (I-I')}{\cos I\cos I'}$	$\frac{N}{N'}\frac{\cos I}{\cos I'}=\cot I\tan I'$
$\frac{\partial U'}{\partial L}$	$=\frac{1}{L-r}\frac{\sin (I-I')}{\cos I\cos I'}$	0
$\frac{\partial U'}{\partial r}$	$=-\frac{L}{r(L-r)}\frac{\sin (I-I')}{\cos I\cos I'}$	0
$\frac{\partial U'}{\partial (N/N')}$	$=-\frac{\sin I}{\cos I'}$	$-\frac{\sin I}{\cos I'}$
$\frac{\partial (L'-r)}{\partial U}$	$=r\frac{\sin I'}{\sin U'}\cot U-r\frac{\sin I'}{\sin U'}\cot U'\frac{\partial U'}{\partial U}$	0
$\frac{\partial (L'-r)}{\partial L}$	$=\frac{N}{N'}\frac{\sin U}{\sin U'}-r\frac{\sin I'}{\sin U'}\cot U'\frac{\partial U'}{\partial L}$	$\tan I\cot I'=\frac{N'}{N}\frac{\cos I'}{\cos I}=\frac{\partial U}{\partial U'}$
$\frac{\partial (L'-r)}{\partial r}$	$=-\frac{N}{N'}\frac{\sin U}{\sin U'}-r\frac{\sin I'}{\sin U'}\cot U'\frac{\partial U'}{\partial r}$	-1
$\frac{\partial (L'-r)}{\partial (N/N')}$	$=\frac{N'}{N}r\frac{\sin I'}{\sin U'}-r\frac{\sin I'}{\sin U'}\cot U'\frac{\partial U'}{\partial (N/N')}$	0.

Examining these equations it will be observed that some combinations of the optical quantities recur. If new letters be assigned to these the above partial differential coefficients will be greatly reduced in form.

Let $$E=r\frac{\sin I'}{\sin U'},\quad F=\frac{N}{N'}\frac{\sin U}{\sin U'},\quad G=\frac{\sin (I-I')}{\cos I\cos I'}.$$

The differential coefficients then become,

For curved refracting surfaces:	For plane refracting surfaces:
$\frac{\partial U'}{\partial U}=1+G\cot U$	$\frac{N}{N'}\frac{\cos I}{\cos I'}$
$\frac{\partial U'}{\partial L}=\frac{G}{L-r}$	0
$\frac{\partial U'}{\partial r}=-\frac{L}{r(L-r)}G$	0
$\frac{\partial U'}{\partial(N/N')}=-\frac{\sin I}{\cos I'}$	$-\frac{\sin I}{\cos I'}$
$\frac{\partial(L'-r)}{\partial U}=E\cot U-E\cot U'\frac{\partial U'}{\partial U}$	0
$\frac{\partial(L'-r)}{\partial L}=F-E\cot U'\frac{\partial U'}{\partial L}$	$\frac{N'}{N}\frac{\cos I'}{\cos I}=\frac{\partial U}{\partial U'}$
$\frac{\partial(L'-r)}{\partial r}=-F-E\cot U'\frac{\partial U'}{\partial r}$	-1
$\frac{\partial(L'-r)}{\partial(N/N')}=\frac{N'}{N}E-E\cot U'\frac{\partial U'}{\partial(N/N')}$	0.

For paraxial rays $E=rI'/U'$, $F=NU/N'U'$, $G=I-I'$. The above differential coefficients then become:

For curved refracting surfaces:	For plane refracting surfaces:
$\frac{\partial U'}{\partial U}=\frac{U'}{U}$	$\frac{N}{N'}$
$\frac{\partial U'}{\partial L}=\frac{I-I'}{L-r}$	0
$\frac{\partial U'}{\partial r}=-\frac{L(I-I')}{r(L-r)}$	0
$\frac{\partial U'}{\partial(N/N')}=-I$	$-I$
$\frac{\partial(L'-r)}{\partial U}=0$	0
$\frac{\partial(L'-r)}{\partial L}=\frac{N}{N'}\frac{U}{U'}-r\frac{I'}{U'}\frac{(I-I')}{L-r}$	$\frac{N'}{N}$
$\frac{\partial(L'-r)}{\partial r}=-\frac{N}{N'}\frac{U}{U'}+\frac{I'L(I-I')}{U'^2(L-r)}$	-1
$\frac{\partial(L'-r)}{\partial(N/N')}=\frac{N'}{N}\frac{rI'}{U'}+\frac{rII'}{U'^2}$	0.

After determining these partial differential coefficients they are used in the usual manner, that is,

$$dU' = \frac{\partial U'}{\partial U}dU + \frac{\partial U'}{\partial L}dL + \frac{\partial U'}{\partial r}dr + \frac{\partial U'}{\partial (N/N')}d\left(\frac{N}{N'}\right),$$

$$d(L'-r) = \frac{\partial (L'-r)}{\partial U}dU + \frac{\partial (L'-r)}{\partial L}dL + \frac{\partial (L'-r)}{\partial r} + \frac{\partial (L'-r)}{\partial (N/N')}d\left(\frac{N}{N'}\right).$$

It must not be forgotten that since these equations were derived by differentiating, they become less and less accurate as the correction to be applied becomes greater and greater, and that the equations fail completely when the points of intersection of the incident and the refracted rays with the axis fall on opposite sides of the refracting surface, a frequent occurrence in optical design. In this case the ray has to be traced through this surface.

It is further to be remembered that these equations are intended for use after an optical design (any optical design since these equations are perfectly general) has been carried well along toward completion and rays have been traced for the final check, and the design found wanting in some respect. Therefore it follows that the work of performing these calculations is much reduced due to the fact that practically all of the quantities appear, with their logs, in the tracing data to which the equations are to be applied, and to the fact that, in these calculations, only the small differences are used, with the consequences that a slide rule can be used without a serious loss of precision. The effect of a given change on the position of the finally refracted ray is thus determined with some saving of time and effort over that required to retrace the rays. It must, however, always be remembered that, at such surfaces where the intersection of the ray with the axis switches from one side to the other of the refracting surface, the ray must be traced through that surface.

Application

For the first example it will be assumed that the index of refraction changes by 0.02429. (1.51851 for borosilicate crown to 1.54280 for ordinary crown. These values are the compromise values for the Conrady three ray method.) The rays were retraced with the new values of the indices of refraction for the purpose of checking the results obtained with these equations. The results for the original tracings after passing through the second surface (the first surface is not involved in a test made on rays parallel to the axis on entering the eyepiece) were as follows:

$\log \sin I = 9.30103^-$	$\log r = 1.00000$
$\log \sin I' = 9.48245^-$	$\log \sin U' = 9.02943$
$\log \cos I' = 9.97899$	$\log N/N' = 0.18142$
$\log \cot U' = 0.96806$	$\log d(N/N') = 8.38543.$

From these we get $\log E = 1.45302$. F and G are not here required. Then

$$dU' = \frac{\partial U'}{\partial (N/N')}d\left(\frac{N}{N'}\right) = \frac{-\sin I}{\cos I'}$$

$$= 0.0050988 \text{ radian or } 17' 31.7''.$$

From the newly traced rays we obtain $17' 32.6''$. Also

$$d(L'-r) = \frac{\partial (L'-r)}{\partial (N/N')}d\left(\frac{N}{N'}\right) = \frac{N'}{N}E + E\cot U'\frac{\sin I}{\cos I'}$$

$$= 0.4540 - 1.3445 = -0.8905.$$

From the newly traced rays we obtain -0.8509.

Note: The discrepancy is here -4.4 percent for a change of -3.1 percent change in N/N'.

For the third surface we carry forward from the last surface

$$dU = 0.005099 \quad \text{and} \quad dL = -0.8905$$

and from the original tracings come

$\log \sin I = 9.02943^-$	
$\log \cos I = 9.99750$	
$\log \cos I' = 9.99892$	
$\log N/N' = -0.18142$	Negative sign means the index is in the denominator.

$\log d(N/N') = 8.01565.$

Then

$$dU' = \frac{\partial U'}{\partial U} dU + \frac{\partial U'}{\partial (N/N')} d\left(\frac{N}{N'}\right)$$

$$= \frac{N}{N'} \frac{\cos I}{\cos I'} dU - \frac{\sin I}{\cos I'} d\left(\frac{N}{N'}\right)$$

$$= 0.003347 - 0.001112$$

$$= 0.002235 \text{ radian} = 7' 41''.$$

From the newly traced rays we get 7′ 30″.

Note: The discrepancy is here 2.5 percent for a change of 4.5 percent in U.

Also

$$d(L' - r) = \frac{\partial (L' - r)}{\partial L} dL = \frac{N'}{N} \frac{\cos I'}{\cos I} dL = -1.5235.$$

From the newly traced rays we obtain −1.5081.

Note: The discrepancy is here −1.01 percent for a −7.7 percent change in L.

For the fourth surface we carry forward from the last surface

$$dU = 0.002235 \quad \text{and} \quad dL = -1.5235$$

and from the original tracings come

log sin $I = 8.0708^-$	log cot $U = 1.1509$
log sin $I' = 8.2522^-$	log cot $U' = 1.1147$
log cos $I = 0.0000$	log $r = 1.2305^-$
log cos $I' = 9.9999$	log $(L - r) = 0.4532$
log sin $U = 8.8480$	log $N/N' = 0.1814$
log sin $U' = 8.8840$	log $d(N/N') = 8.3854$.

From these we get log $E = 0.5987$, log $F = 0.1454$, log $G = 7.7857$. Then

$$dU' = (1 + G \tan U) dU + \frac{G}{L - r} dL - \frac{\sin I}{\cos I'} d\left(\frac{N}{N'}\right)$$

$$= -0.0005623 \text{ radian} = -1' 56''.$$

From the newly traced rays we obtain −2′ 52″.

Note: The discrepancy is here −33 percent for a −3.2 percent change in U.

Also

$$d(L' - r) = \{E \cot U - E \cot U'(1 + G \tan U)\} dU + \left\{F - E \cot U' \frac{G}{L - r}\right\} dL + \left\{E \frac{N'}{N} + E \cot U' \frac{\sin I}{\cos I'}\right\} d\left(\frac{N}{N'}\right),$$

$$= -1.911.$$

From the newly traced rays we obtain 1.970 − 3.969 = −1.999.

Note: The discrepancy is here −4.4 percent for a −10 percent change in L.

It will be observed that large changes in U and L produce results considerably in variance with the correct values. These discrepancies are, however, not cumulative. A surface often corrects the discrepancy introduced by a previous surface. In this case, the agreement in U' for the second surface is excellent while that for L' is poor. For the fourth surface the condition is just the reverse, the large discrepancy in L' at the second surface has been completely eliminated at the fourth and the angle, in which case the agreement was excellent at the second surface, has accumulated a rather large discrepancy at the fourth surface. This is a common behavior of these equations, but even where the discrepancy grows to considerable magnitudes the equations are still very useful in indicating the kind and amounts of correction of the prescription desirable. It might be of interest to state that while the writer has made some considerable use of these equations, the results here are the worst he has run across. It is also well to keep in mind that for changes of U and L smaller than those here used the agreement becomes very rapidly better.

A Complete Analysis of a Special Case

This analysis would not be complete without examining a particular prescription more completely, not only for the aberrations so far examined but for the other monochromatic off axis or oblique aberrations. We will choose for this final analysis the following prescription:

Borosilicate crown	Ordinary crown
∞	∞
1.500000 mm	1.500000 mm
10.00000 mm	10.00000 mm
26.00108	25.15867
∞	∞
2.550000 mm	2.550000 mm
17.00000 mm	17.00000 mm

The ray tracings give the following results:

Quantities	Borosilicate crown	Ordinary crown	Percent change
d'	26.00108	25.15867	−3.33
U_y'	4° 23′ 27.01″	4° 30′ 59.70″	2.86
u_y'	0.07715099	0.07948328	2.94
u_v'	0.07699815	0.07926792	2.95
L_y'	−13.03104	−13.24834	1.66
l_y'	−11.28318	−11.45721	1.55
l_v'	−11.86944	−12.08647	1.79
Y	2.000000	2.000000	0.00

(*Note:* The above results were obtained to the full precision of seven places in the index of refraction simply to insure the absence of computing errors in the sixth place. Since, however, the index of refraction is not generally known to even the sixth place and, further, since the glass shop does not in general adjust d' closer than a few thousandths of a millimeter, the last two places above have little practical value though important in theoretical investigations.)

From the above data the following results are obtained:

Quantities	Borosilicate crown	Ordinary crown	Percent change
O.S.C.′	0.00117227	0.00124024	5.8
f_0'	196.22	169.05	−13.3
f_e'	25.9232	25.16252	−2.93
MA'	7.56946	6.7104	−11.3
g_7	0.0009997	0.0010017	0.20
Sep. coef.	1.063139	1.074718	24.2
Air S. coef.	1301.	1126.	−13.4

(*Note:* The effects on the adjustment coefficients will be useful in adjusting prescriptions by the empirical method.)

Interesting conclusions may be drawn from these data.

Changes in the index can be made without concerning ourselves about the Coma as there will be little change, so long as we satisfy the conditions called for by the empirical method described in this article.

The focal length of the objective which must be used with each eyepiece, however, changes very markedly.

The focal length of the eyepiece itself is not much effected.

The borosilicate crown glass gives a higher over-all magnification than ordinary crown glass, largely due to the increase in f_0'.

The transverse chromatic aberration was made the same in both cases.

Changes in the prescription to permit a given change of the index of refraction can easily be made, within reasonable limits, from the above table, and the probable changes in the various other quantities given can also be calculated.

CHANGES OF THE CHROMATIC ABERRATION WITH d' CONSTANT

It will be noted that d' (the separation of the components of the eyepiece) has to be changed in order to hold the transverse chromatic aberration constant. It might be of interest to know how much the chromatic correction would be disturbed if the d' were not changed. Retracing the rays for the ordinary crown but with the same value of d' as was used in the case of the borosilicate crown gave the following data.

$$\begin{aligned} \text{O.S.C.}' &= 0.00114701 \\ f_0' &= 159.60 \\ f_e' &= 26.1222 \\ MA' &= 6.1097 \\ g_7 &= 0.000347. \end{aligned}$$

It will be observed that the chromatic correction (indicated by the low value of g_7) has been greatly affected by a change in d' of only 0.8 of a millimeter.

CHANGES CAUSED BY A CHANGE IN THE THICKNESS OF THE LENSES

For the rays traced parallel with the axis and incident on the eye lens of the eyepiece there is no effect produced on the final image by changing the thickness of the eye lens. The effect of changing the thickness of the field lens only will therefore be examined. Tracing the axial rays for $d' = 25.00520$ for the borosilicate crown glass and for a focal length ratio of 1.7 gives, for a 10 percent reduction in the thickness:

Quantities	Borosilicate crown	Ordinary crown	Percent change
t	2.55000	2.29500	−10.0
U_y'	4° 23′ 24.23″	4° 25′ 17.32″	
u_y'	0.07713796	0.07766910	
u_v'	0.07698471	0.07752955	
L_y'	−13.039111	−12.713243	
l_y	−11.290626	−10.989200	
l_v	−11.877134	−11.566776	
Y	2.000000	2.000000	

From these data the following results are obtained:

t	2.55000	2.29500	−10.0
O.S.C.′	0.00117186	0.00118866	1.43
f_0'	196.14	198.73	1.32
f_e'	25.927	25.7503	.68
MA'	7.5652	7.7177	2.01
g_7	0.0009968	0.0011031	10.7

The changes produced by this 10 percent reduction in the thickness of the field lens are given in the last column. It will be noted that the chromatic correction is ten times more sensitive than is the coma correction to these changes in thickness of the field lens, but even then, the effects are not large so that moderate changes in the thickness can be made without serious consequences.

In concluding this article, it will be desirable to get a complete mental picture of the properties of a lens designed according to the procedure heretofore described. With that in view all the data on the particular eyepiece previously examined in part together with the oblique aberrations yet to be computed will be assembled under the following head.

THE PROPERTIES OF A PARTICULAR HUYGENS EYEPIECE

The prescription:

∞

1.5000 mm

10.000 mm

26.00108 mm

∞

2.5500 mm

17.000 mm

Focal length of the eye lens (f_A'),

$$R_2/(N_y-1)=19.2860.$$

Focal length of the field lens (f_B'),

$$1.7\times 19.2860=32.7862.$$

Focal length ratio, 1.7.

Focal length of the eyepiece as a whole,

$$\frac{f_A'f_B'}{f_A'+f_B'-a}=25.923.$$

Focal length of the objective with which this eyepiece must be used to realize the corrections here given (see Eq. (10)), 196.22 mm.

Thickness of the eye lens, 1.5000 mm.

Thickness of the field lens, 2.5500 mm.

Positions of the Gaussian planes:

Eye lens

$$\text{Anterior, } t_A/N_y=0.98781 \text{ mm,}$$

$$\text{Posterior, } \frac{t_AR_2}{N(R_1-R_2)-(N-1)t_A}=0.$$

Field lens

$$\text{Anterior, } t_B/N_y=1.67928,$$

$$\text{Posterior, } -\frac{t_BR_4}{N(R_3-R_4)-(N-1)t_B}=0.$$

The positions of the Gaussian planes for the eyepiece as a whole:

$$\text{Anterior, } H_AH=\frac{af_A'}{f_A'+f_B'-a}=21.8862,$$

$$\text{Posterior, } H'H_B'=\frac{af_B'}{f_A'+f_B'-a}=37.2065.$$

Note: See Fig. 1 for a clearer understanding of the above quantities.

A semi-aperture of 2 mm will be assumed.

Tracing the standard rays through the eyepiece, parallel to the axis and according to the prescription given and with indices 1.51851 and 1.52652, the following data are readily obtained.

Directly from the tracing data,

Spherical aberration = 1.7479 mm.

Longitudinal chromatic aberration = 0.5863 mm.

The extent of the aberrations are sought at 14°. In order to determine these from traced rays, it will be necessary first to determine the angle the incident principal ray makes with the axis of the system. The perfect optical theory gives us,

$$\tan x=-\frac{f_e'}{f_0'}\tan 14°$$

$$=-\frac{25.923}{196.22}\times 0.24833=1°\ 53'\ 12''.$$

Tracing two rays, one in y and the other in v, from the objective end of the system gives

actual $U_{prA}=-14°\ 23'\ 14''$ for the y ray,

$-14°\ 23'\ 17''$ for the v ray,

from which it follows that

the percent distortion

$$=100\left(1-\frac{\tan \text{ actual } U'_{prA}}{\tan \text{ ideal } U'_{prA}}\right)=-2.88$$

and

transverse chromatic aberration

$$=1-\frac{\tan U'_{prv}}{\tan U'_{pry}}=-0.0002.$$

Tracing two rays, one at the top and the other at the bottom of the aperture and with the index for the y ray and for the angle 14° 23′ 14″, the following data are obtained:

$$\begin{aligned} L_u' \text{ (upper)} &= 46.778 \text{ mm}, \\ L_l' \text{ (lower)} &= -170.43 \text{ mm}, \\ U_u' \text{ (upper ray)} &= 6° \ 13' \ 25'', \\ U_l' \text{ (lower ray)} &= -2° \ 23' \ 22'', \end{aligned}$$

from which the following quantities are obtained

$$H'_{ul}=\frac{(L_l'-L_u')\sin U_u'}{\sin (U_u'-U_l')}\sin U_l'=6.556 \text{ mm}.$$

See Fig. 2.

$$\begin{aligned} L'_{ul}&=L_l'-\frac{(L_l'-L_u')\sin U_u'}{\sin (U_u'-U_l')}\cos U_l' \\ &=L_u'-\frac{(L_l'-L_u')\sin U_l'}{\sin (U_u'-U_l')}\cos U_u' \\ &=-170.43+157.10=-13.33, \end{aligned}$$

where H'_{ul} is the distance of the final image from the axis and L'_{ul} the distance from the foot of the perpendicular, dropped from the focal point of the u and l rays to the axis, and the pole of the last surface.

With these quantities given, together with the point of intersection of the traced marginal ray, which entered the eyepiece parallel to the axis, L', it is now possible to compute all the other oblique aberrations (in the object space when the eyepiece is in use) as follows:

The tangential curvature of field:

$$X_T'=L'_{ul}-L'=-13.33+13.03=-0.30 \text{ mm}.$$

This is a little more than half the amount for which Conrady says the eye can easily accommodate.

The tangential coma,

$$\begin{aligned} \text{Coma}_T' &= (L'_{pr}-L')\tan U'_{pr}-H'_{ul} \\ &= (196.22+25.92-37.21+13.33) \\ &\quad \times \tan (1° \ 53' \ 12'')-6.556 \\ &= -0.025 \text{ mm}. \end{aligned}$$

The sagittal coma,

$$\text{Coma}_S'=\frac{-0.025}{3}=-0.0083 \text{ mm},$$

$$\text{O.S.C.}'=-\frac{0.0083}{6.56}=-0.00127.$$

The Petzval curvature,

$$X'_{ptz}=-\tfrac{1}{2}H'^2\sum\frac{(N-1)}{N}C=-1.1653.$$

The negative sign indicates curvature to the left or a "round" curvature for left to right tracing. The fact that X_T' is smaller than X'_{ptz} indicates negative astigmatism, determined as follows:

The distance of the tangential curve from the Petzval is $-1.16-(-0.30)=-0.86$ mm.

The distance of the sagittal curve from the Petzval curve is one third of that or -0.29 mm.

The astigmatism is, therefore, -0.57 mm a very favorable amount.

In concluding this article, it will be interesting to examine this particular eyepiece by means of the Taylor equations in order to see how well these equations predict the performance of this type of optical system. The results just given have been calculated solely from the final results of a set of rays traced completely through the system, and with the aid of Conrady's "Closing equations" in which the only approximations made are those resulting from the interchange of angles, sines, and tangents of relative small angles.

The most serious of the approximations made in the use of Taylor's equations is the use of the first-order thin lens equation for determining the eccentricity constant. This point will be examined in detail by determining the eccentricity constant in three ways. Under the column headed "Trace" this constant will be determined from tracing data thus involving no approximations at all.

The second, headed "Exit pupil," will be in accordance with the usual practice, that is by using the thin lens formula and starting at the exit pupil. The third method, headed "Entrance pupil," again used the first-order lens equation but this time we start at the entrance pupil of the system, assuming the light travelling in its normal direction through the eyepiece.

The following table gives the positions of the image planes for the exit (entrance pupil for the tracing operations) and entrance (exit pupil for ray tracing operations) pupil, computed in these three ways.

	Trace	Exit pupil	Entrance pupil
X_A	−6.435	−6.425	−7.461
X_A'	−9.886	−9.657	−12.170
X_B	−37.566	−37.337	−39.850
X_B'	+184.93	+269.0	+184.93

Note: The *A* lens is the eye lens and the *B* lens is the field lens in the above table.

With these values of the X's the calculations are carried out in the usual way. It must, however, be remembered that some of Conrady's aberrations are calculated for the exit pupil, others for the entrance pupil and the Taylor equations here used give all results as seen from the exit pupil. Furthermore Taylor's results are expressed in radians while Conrady's are linear. When all these conditions are fully considered and all values for both systems are transfered to the exit pupil and making the changes in some cases due to the fact that the measures used by Taylor and by Conrady are not the same, and therefore changing them all to the Taylor system, we arrive at the following results:

	Trace	Exit pupil	Entrance pupil
Angular transverse chromatic aberration			
Taylor	7.2″	2.7″	49.8″
Conrady	3″		
Distortion			
Taylor	−2.42%	−2.39%	−2.75%
Conrady	−2.88%		
Tangential coma			
Taylor	−0.00109 rad.	−0.00114 rad.	−0.00199 rad.
Conrady	−0.00090 rad.		
Primary curvature			
Taylor	−0.00212 rad.	−0.00254 rad.	−0.00896 rad.
Conrady	−0.00178 rad.		
Petzval curvature			
Taylor	−0.00689 rad.		
Conrady	−0.00684 rad.		
Astigmatism			
Taylor	−0.00308 rad.	−0.00280 rad.	−0.01045 rad.
Conrady	−0.00338 rad.		

The agreement is, therefore, quite satisfactory except when the X's are computed from the entrance pupil end.